# 6.04 Mapping Peatlands in Boreal and Tropical Ecoregions

**LL Bourgeau-Chavez, SL Endres, and JA Graham,** Michigan Technological University, Ann Arbor, MI, United States
**JA Hribljan, RA Chimner, and EA Lillieskov,** Michigan Technological University, Houghton, MI, United States
**MJ Battaglia,** Michigan Technological University, Ann Arbor, MI, United States





## 6.04.1 Introduction

Peatlands are a class of wetlands that are defined as having saturated soils, anaerobic conditions, and large deposits of partially decomposed organic plant material (peat). Occurring in ecozones from the tropics to the arctic, peatlands are estimated to cover just under 4.5 million km$^2$, roughly 3–5% of the Earth's land surface (Maltby and Proctor, 1996). Although they cover a small amount of land globally, peatlands are estimated to store ~30% of the Earth's soil carbon (C) (Gorham, 1991; Botch et al., 1995; Lappalainen, 1996; Zoltai and Martikainen, 1996; Clymo et al., 1998; Moore et al., 1998; Yu et al., 2010; Page et al., 2011), making them crucial to the global C cycle. Therefore, it is vital to obtain improved estimates of peatland distribution across the globe, as well as to monitor disturbances due to climate change or human activity. Efforts to map global wetlands from MODIS or other coarse resolution optical sources are ineffective in detecting and mapping peatlands. With coarse (250 m–1 km resolution) data, peatlands typically are grouped with a more general wetland class. Since peatlands are often small and interspersed with upland and other wetland types, it is essential to use finer resolution data (~30 m or better) to distinguish peatland types as described further in this article. Advanced remote sensing methods that use a combination of data sources and imagery from multiple seasons are necessary to capture the hydrologic and phenological variation that characterizes the diversity of peatlands that exist on the landscape. This article reviews the need for peatland mapping in boreal and tropical systems and summarizes applications of remote sensing for this purpose. Before mapping any landscape, it is necessary to have an understanding of the systems to be mapped. Knowledge of the characteristics of the ecosystems allows for informed decision making when choosing the combination of remote sensing data sources to best distinguish and classify the region of interest. In this article, we begin with background information on peatlands, followed by a review of mapping approaches from the literature and lastly, provide three examples of using multisensor, multitemporal optical, and radar data for mapping peatlands. The multisensor and multidate approaches are shown through examples to be more effective than using a single date of imagery and/or a single sensor.

### 6.04.1.1 How Does Peat Form

For peat to accumulate, the long-term rate of primary production must be greater than the rate of decomposition and losses from other sources such as wildfire and dissolved carbon export (Wieder and Lang, 1983; Vitt, 2006). Although production and decomposition rates vary considerably between boreal, alpine, and tropical peatlands, a production–decomposition imbalance is required for peatland persistence. Peat is formed from a range of plant types, including both bryophytes: *Sphagnum*, feather, and brown-mosses; and vascular plants: cushion plants, ericaceous shrubs, graminoids, palms, and trees. Peat is characterized



Comprehensive Remote Sensing, First Edition, 2018, 24–44

as water-logged, anoxic, and often composed of recalcitrant plant litter, lending to particularly slow decomposition rates (Moore et al., 2007). In comparison to other ecosystems, northern peatlands have low productivity (Frolking et al., 1998; Moore et al., 2002), and low temperatures and anoxic conditions greatly inhibit decomposition, allowing peat to form. Scientists initially believed that peatlands could only be formed in colder climates (Moore and Bellamy, 1974), reasoning that in warmer temperatures the rate of decomposition would outpace plant production (Lloyd and Taylor, 1994; Raich and Potter, 1995; Fang and Moncrieff, 2001). Rather, tropical peatlands have demonstrated rapid peat accumulation rates, averaging 1–5 mm $yr^{-1}$ and up to 10 mm $yr^{-1}$ (Chimner and Karberg, 2008; Lähteenoja et al., 2009), much faster than temperate and boreal peat accumulation rates that are typically less than 1 mm $yr^{-1}$ (Gorham, 1991). Although annual tropical production rates are generally high and much of the litter is easily decomposed, it has been suggested that lowland tropical peat is the result of the slow decomposition of woody material (Chimner and Ewel, 2005), while boreal peat is formed from mosses, graminoids, and woody material.

The accrual of peat over millennia leads to the formation of deep peat deposits, which may reach depths as great as 15–20 m below the surface (Anderson, 1983; Clymo et al., 1998; Limpens et al., 2008; Turunen et al., 2002). Although the maximum depths of some peat deposits are remarkable, there are some international inconsistencies regarding the minimum peat thickness required for an ecosystem to be classified as "peatland." In some countries thirty centimeters of peat is the minimum depth required for an ecosystem to be defined as a peatland (Joosten and Clarke, 2002; Rydin and Jeglum, 2013); however, the two peat rich countries, Russia and Canada, use a peat thickness of 50 and 40 cm, respectively, in national peatland inventories, (National Wetlands Working Group, 1997; Loisel et al., 2017) which may complicate global peat estimates.

### 6.04.1.2 Global Peatland Distribution

Peatlands occur from the tropics to the arctic, covering 3–5% of the Earth's land surface (Maltby and Proctor, 1996), spanning approximately $4.0 \times 10^6$ $km^2$ in the northern hemisphere and $4.5 \times 10^4$ $km^2$ in the southern hemisphere (Yu et al., 2010). However, a majority of the Earth's peatlands exist in the boreal regions of the northern hemisphere. Of the boreal forest region, 25–30% of the landscape is peatland (Gorham, 1991; Wieder et al., 2006). Tropical peatlands account for around 11% of all peatland area at current estimates of $4.41 \times 10^5$ $km^2$ (Page et al., 2011). The largest expanses of tropical peatlands are located in lowland areas of Southeast Asia, especially Indonesia (Rieley et al., 1996; Page et al., 2011), and in the Amazon basin (Lähteenoja et al., 2009). Africa's lowland peatland area is largely unknown, except for the Congo Basin, where recent studies estimate peatland area at $1.45 \times 10^5$ $km^2$ (Dargie et al., 2017). Peatlands are also located at high elevations in most mountain ranges (Cooper et al., 2012). Tropical alpine peatlands are numerous in the Andes, many tropical islands, and in Africa (Smith and Young, 1987; Chimner, 2004; Chimner and Karberg, 2008).

Six countries (boreal Russia, Canada, USA, Finland, Sweden, and tropical Indonesia) together account for 93% of all known peatland area (Joosten and Clarke, 2002; Wieder et al., 2006). Southern hemisphere peatlands are far less abundant, perhaps owing to limited land with appropriate conditions for peatland initiation and development (Gore, 1983). Outside of the tropics, southern hemisphere peatlands are most plentiful in Patagonia and Tierra del Fuego with rare occurrences in Australia and islands outside the Antarctic Circle (McGlone, 2002; Yu et al., 2010). With the large distribution of peatlands across a range of landforms, latitudes, and elevations, it is no wonder that peatlands encompass a large array of types, with varying degrees of species richness and hydrological conditions.

### 6.04.1.3 Peatland Classification Schemes

Boreal peatland types can be classified along chemical, botanical, and hydrological gradients (Zoltai and Vitt, 1995; Bridgham et al., 1996). Perhaps the most common peatland classification system is based on the chemo-hydrological distinction of bog from fen. Due to an accumulation of peat, the growing ground layer of bogs becomes elevated above the water table and are distinguished from fens by being ombrotrophic, i.e., they receive almost all their water and associated nutrient and mineral input from precipitation. Conversely, fens are minerotrophic, i.e., they receive ground and surface water inputs (Drexier et al., 1999), resulting in more nutrient and mineral availability in fens.

Of the peatland classes, bogs are generally the most acidic, nutrient poor, furthest removed from the water table, and possess relatively low species richness. To maintain adequate moisture to facilitate growth, bogs only develop in areas where precipitation is greater than potential evapotranspiration and droughts are rare (Maltby and Proctor, 1996). In boreal bogs, the roots of ericaceous shrubs provide a lattice for dense populations of *Sphagnum* mosses to retain moisture at levels far above the water table (Malmer et al., 1994). Although nitrogen has been thought to be the limiting growth factor to *Sphagnum*, the primary peat former in boreal bogs and poor fens (Limpens et al., 2006), it may be that water and nitrogen are colimiting factors along a distance-to-water table gradient (Graham and Vitt, 2016).

As fens are not solely dependent on precipitation, they are not restricted to areas of high precipitation and can form in any region that has regularly saturated soils, such as river basins, topographic depressions, and ground water discharge zones (Maltby and Proctor, 1996). Fens are further divided along the chemical, botanical, and hydrological gradients, with poor fens being the closest to bog. Like bogs, poor fens typically have full groundcover of *Sphagnum* moss, have a pH less than 5.5, share many plant species, but are not fully elevated above the water table and do receive some water input from surrounding landscapes. While bogs are restricted to the lowest end of the chemical gradients, fens have a wider range and higher levels of pH as a result of varying conditions of incoming groundwater chemistry and the geologic setting of the watershed (Chimner et al., 2010).

Mixed with upland ecosystems, these different boreal peatland types often neighbor each other across the landscape, resulting from the complexity of both abiotic and biotic factors (Vitt et al., 2003; Graham et al., 2015). Over long periods of time, peatland types can change as a result of successional processes (Glaser, 1981). One common pathway is ombrotrophication, where peatlands transition from minerotrophy to ombrotrophy by peat formation and accumulation to the point that the ground layer becomes isolated from groundwater and surface runoff (Charman, 2002). When the water-logged edge of a peatland encroaches upon the surrounding landscape peatlands commonly spread in a process called paludification (Kuhry and Turunen, 2006).

In addition to the chemo-hydrologic gradients, peatlands differ in vegetation cover. For the purposes of mapping, one of the most important differences is the presence or absence of trees **Fig. 1**. Open, nonforested peatlands can be dominated by *Sphagnum*, low ericaceous shrubs, and sedges. Boreal to temperate peatlands can also be dominated by low diversity forests of the Pine family (Pinaceae) with *Picea*, *Pinus*, and *Larix*, being especially important genera. At higher pH levels, these peatlands can be dominated by other conifers (e.g., *Thuja*).

Peatlands existing in tropical regions are located in lowland and high-elevation landscapes. For southeast Asia, which contains 77% of tropical peat (Page et al., 2011), three classes of peatlands have been suggested: coastal peatlands, basin or valley peatlands, and the high-elevation peatlands (Rieley et al., 1996; Page et al., 1999). These divisions are based on peatland location, formational pathway, and age of peat deposits (Page et al., 2006).

Low-elevation (basin or valley) tropical peatlands are generally angiosperm tree or palm dominated with limited bryophyte cover, forming what are known as peat swamp forests. Tree biodiversity is much higher in tropical than boreal lowland peatlands. Over 200 tree and palm species occupy tropical peat swamps in Indonesia alone. In contrast, pan-boreal peatlands contain less than two dozen tree species (Wieder et al., 2006). Above-ground production in tropical peat swamp forests can exceed 1100 g C $m^{-2}$ $yr^{-1}$, but high decomposition rates of plant litter prevent it from accumulating as peat (Chimner and Ewel, 2005). Unlike boreal and temperate peatlands, where peat is predominately formed from above-ground production, tropical lowland peat is formed mostly from fine roots, branches, and trunks, creating a fibrous woody peat (Anderson, 1983; Page et al., 1999).

High-elevation tropical peatlands, 3500 m a.s.l. in the Andes Mountains (**Fig. 1**), may form in areas of restricted drainage from the presence of cushion plants, which can form the bulk of peat and create conditions favoring continued peat formations (Sklenar and Jorgensen, 1999; Fritz et al., 2011; Benavides et al., 2013; Hribljan et al., 2017). High-elevation peatlands can form in areas which receive perennial overland and groundwater inputs. In Peru, the term "bofedales" meaning wetlands with peat layers is used. Bofedales exist in areas that receive water from melting glaciers, rivers, lakes, and groundwater in addition to precipitation. They are important sources of water and forage for livestock and represent hotspots of biodiversity (Ruthsatz, 2012).

### 6.04.1.4 Why Peatlands Are Important to the Carbon Cycle

The result of the accumulation of peat over millennia has been the immense sequestration of global carbon in peatlands, despite their low abundance on the Earth's landscape. Recent estimates of the total peatland C pool is ≈ 612 (530–694) Gt C (Yu et al.,

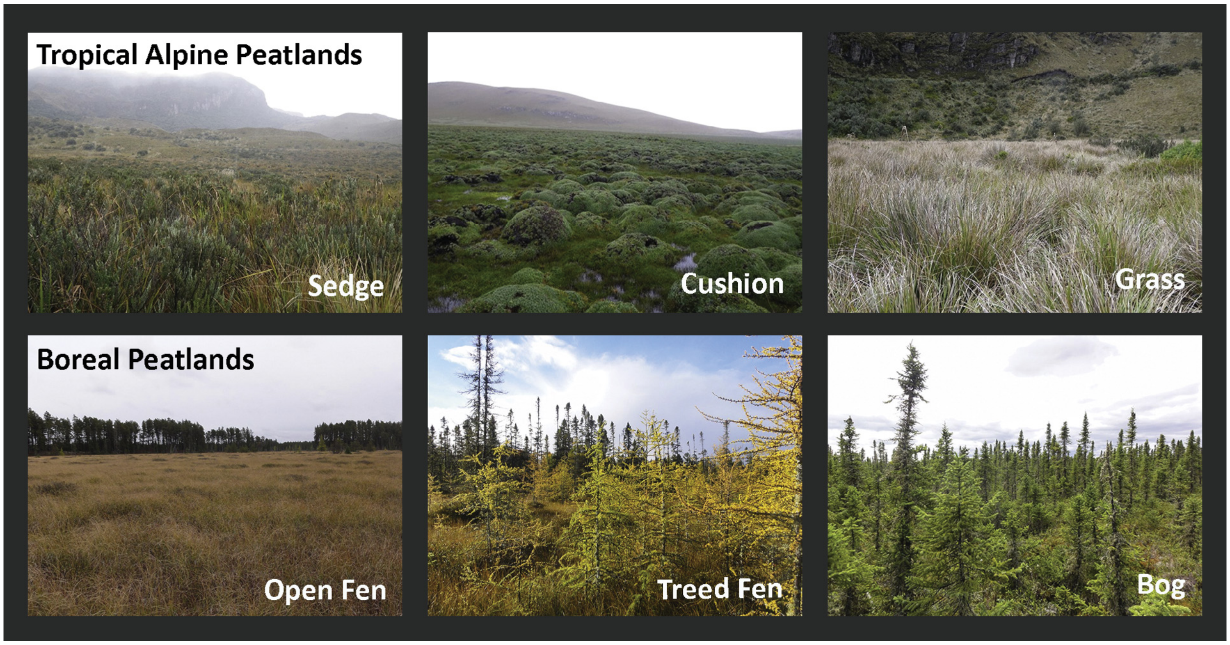


**Fig. 1** *Top row*: Photos of peatlands in Ecuador showing sedge, cushion, and grass tropical alpine peatland types; and *bottom row*: photos of peatlands in boreal Canada showing an open fen, treed fen, and wooded bog.

2010), and potentially as high as 728 Gt C when including the most recent tropical estimates ($\approx$ 88.6 Gt C from Page et al., 2011). This slightly surpasses that of estimated global vegetation ($\approx$ 560 Gt C) and is slightly less than that of C in the atmosphere ($\approx$ 850 Gt C from IPCC, 2013; Turetsky et al., 2015). Of global peatlands, northern hemisphere peatlands have been estimated to contain around 89% of C stocks while tropical peatlands are estimated to contain 8%, and southern hemisphere (nontropical) peatlands 2% of C stocks (Yu et al., 2010). However, newer studies have found tropical peatlands may contain up to 19% of the global peatland stocks (Page et al., 2011). Although boreal peatlands store more carbon in total, tropical peatlands store more carbon stocks per area (Donato et al., 2011).

Accurate measurements of peatland carbon storage are dependent upon several key variables: the volume of peat, as a function of the area and depth of peatland; the bulk density of peat (dry peat mass per $cm^3$); and the carbon concentration of peat. Inaccuracies arise in peatland C stock estimates due to uncertainties in defining peatlands and their spatial extents, heterogeneous peat depths (Bauer et al., 2003; Fyfe et al., 2014), variable bulk density (Clymo et al., 1998; Turunen et al., 2002), and differences in carbon concentrations (Chimner et al., 2014). Throughout northern peatlands, mean peat C concentration is $\sim$47%, and ranges from 30% to 60% with the lowest C concentrations in *Sphagnum* peat and highest values in herbaceous and woody peat (Loisel et al., 2014). Peat carbon concentration from lowland tropical peatlands generally ranges from 40% to 62% with a mean of 54% C (Page et al., 2011). High-elevation cushion plant dominated tropical peatlands in the Ecuadorian Andes were lower, with values ranging from 14% to 36% C (Chimner and Karberg, 2008). Bulk density and carbon concentrations can vary considerably both along a depth profile and along horizontal gradients.

Throughout the duration of the Holocene peatlands have been a considerable carbon sink (Charman et al., 2013). Long-term rates of C accumulation during the Holocene are 18.6 g $m^{-2}$ $yr^{-1}$ for northern peatlands, 12.8 g $m^{-2}$ $yr^{-1}$ for tropical peatlands, and 22.0 g $m^{-2}$ $yr^{-1}$ for southern peatlands (Yu et al., 2010). In addition to accumulating and storing large stocks of carbon, the vegetative inputs to peat contain nitrogen as well, indicating that peatlands also sequester a significant amount of global nitrogen. Estimates of northern peatland nitrogen storage are 10–13 Gt N (Moore et al., 2005; Loisel et al., 2014), around 9–16% of the global nitrogen pool (Limpens et al., 2006). Numbers of this magnitude suggest that peatlands have a significant role in the global nitrogen cycle as well, and could even limit nitrogen availability globally (McLauchlan et al., 2015; Loisel et al., 2014).

### 6.04.1.5 Biodiversity in Peatlands

In addition to acting as global carbon sinks, peatlands also offer habitat to a variety of flora and fauna. Compared to other peatland types, tropical peat swamp forests have the greatest diversity of flora. Between 30 and 122 different tree species greater than 10 cm in diameter have been recorded in Southeast Asian peat swamp forests (Posa et al., 2011). Yule (2010) highlights the diversity of fish, aquatic invertebrates and flora, and the interesting adaptations of terrestrial flora to these extreme environments. Notably, several large vertebrates are using these ecosystems as a refuge from regional disturbances, including elephants, tapirs, several wild cats, orangutans, proboscis monkeys, and rhinoceros (Yule, 2010).

Peatlands offer a great variety of habitats due to their internal diversity and a diversity of birds can be found throughout peatlands depending on forest cover (Kouki et al., 1992). This internal diversity provides a beneficial space for species that need different environments to complete their lifecycle, such as a carabid beetle living on top of the dry hummocks of boreal peatlands in the winter and in the damp *Sphagnum* lawns in the summer (Främbs, 1994). Woodland caribou in Canada have been found to prefer peatland habitats over other land types, perhaps as a refuge from predators (Rettie and Messier, 2000). Amphibians, reptiles, birds, and arthropods inhabit peatlands but are affected by the presence of pools, nutrient availability, acidity, and soil drainage (Smits et al., 2002; Poulin et al., 1999; Mazerolle, 2001). The diversity of microhabitats in peatlands increases with size, so larger peatlands tend to be more species-rich (Calmé and Desrochers, 2000).

### 6.04.1.6 Threats to Peatlands

As we, and the planet, accelerate from the Holocene to the Anthropocene, many critical changes can be expected to the functional systems of the Earth (Steffen et al., 2007). Arctic and boreal regions, where the bulk of peatlands exist, have been and are predicted to continue to be among the areas most strongly affected by rising temperatures and also changes in precipitation (Chapin et al., 2000; Meehl et al., 2007; IPCC, 2014). The close relationship of water to the functioning of peatlands makes them particularly vulnerable to rapidly changing climatic regimes and disturbances that may significantly alter the water table such as wildfire and land use change. Frolking et al. (2011) predict that the most significant climate impacts on peatlands will be water drainage, particularly in the tropics, while thawing of permafrost and increased fire intensity and frequency will be a threat in the boreal as a result of both drier conditions and drainage. There are numerous other threats facing existing peatlands, including peat extraction, forest cutting, road construction, reservoir creation, oil sands mining, pollution, clear-cutting, and land-use change.

The draining of peatlands results in considerable emissions of $CO_2$ and $N_2O$ and has been particularly exemplified in Southeast Asia (Joosten, 2009). The lowering of the water table increases the exposure of accumulated peat to aerobic environments resulting in more rapid decomposition, though the long-term effects are difficult to predict (Laiho, 2006). In Southeast Asia, peatlands converted to Acacia and oil palm farms have resulted in considerable peat oxidation and subsidence, and subsequent large carbon emissions (Hooijer et al., 2012).

The thawing of permafrost results in the exposure of previously preserved peat to microbial decomposition resulting in carbon release, which may create positive feedback $CO_2$-mediated rising temperatures (Schuur et al., 2008; Dorrepaal et al., 2009). The precise future carbon balance of warming permafrost peatlands remains unknown, yet they remain exceptionally sensitive to continuing changes in the climate (Turetsky et al., 2007). Within the entirety of the northern circumpolar permafrost region, it has been estimated that up to 50% of the belowground soil organic C pool is harbored (Tarnocai et al., 2009).

Wildfire is a common disturbance in some peatlands and temporarily changes peatlands from C sinks to sources (Wieder et al., 2009), yet large peat C stocks stored at depth have been protected from burning by saturated conditions (Turetsky et al., 2015). However, as a result of drying from climate change, wildfires are expected to become more frequent and more intense, and coupled with lower water levels, deeper stores of peat could be vulnerable to burning (Turetsky et al., 2015). Furthermore, particulate matter from peat fires has a negative impact on air quality, which has detrimental effects on human health (See et al., 2007).

Peatlands in tropical regions have been rapidly converted for timber production as well as agricultural products such as palm oil (Koh et al., 2009), which has resulted in increased fires (Cochrane, 2003), drainage (Hooijer et al., 2012), and deforestation (Miettinen et al., 2011). Changes such as these have resulted in large quantities of carbon released to the atmosphere and highlight the importance of the carbon storage in peatlands (Van der Werf et al., 2009; Page et al., 2011).

The persistence of peatlands as a carbon sink depends on the simple balance of primary production exceeding that of decomposition and losses from wildfire, disturbance, or dissolved carbon export, although these processes are dependent on numerous interacting factors. Comprehensive models predict that globally peatlands may continue to act as a C sink, but these models have considerable uncertainty (Charman et al., 2013). Remote sensing provides a method for mapping the existing peatland distribution and monitoring changes through time, including successional trends, as well as climatic and anthropogenic-induced change.

## 6.04.2 Review of Peatland Mapping Approaches

In general, wetlands are difficult to map and monitor using optical imagery alone, especially when they are covered by a closed canopy of vegetation (Wieder et al., 2006) or embedded in complex steeply sloping mountain terrain. Synthetic aperture radar (SAR) microwave energy is capable of penetrating a forest canopy and detecting inundated or wet soils beneath the vegetation, thus improving wetland mapping capability, particularly when combined with optical imagery. SAR is an active sensor, emitting microwave radiation and measuring the energy backscattered from the elements being imaged (e.g., wetland plants). LiDAR (light detection and ranging) data have also been used to detect water beneath a canopy using the intensity of the return (Lang, 2009). In addition, others have used LiDAR-derived DEM products to detect wetland depressions (Wu et al., 2014; Bourgeau-Chavez et al., 2016). More and more, researchers have been utilizing multiple sensors (thermal, optical, LiDAR, and SAR), ancillary datasets (e.g., DEM, and precipitation), and multiple seasons of imagery to better detect wetlands. The use of sensor fusion techniques across multiseasonal datasets has enabled species-specific mapping of vegetation, which is often assumed to be best detected with hyperspectral data. Using multiple seasons of data allows improved discrimination of wetland types by assessing the seasonal variations in phenology related to changes in plant structure and chlorophyll concentrations as well as seasonal patterns of inundation/soil moisture.

Peatlands develop and persist under a complex set of interacting regional and local factors. The type of peatland that develops at a site is a function of the specific hydrologic regime, climate, chemistry, landform, substrate, vegetation, and in high northern latitudes the presence or absence of permafrost (Vitt, 2006). Some of these variables can be used to identify peatlands in the field and in remotely sensed imagery (e.g. hydrologic regime, vegetation, and landform). SAR sensors have been demonstrated to be sensitive to biomass and moisture condition of the canopy and ground layers of vegetated landscapes (Hess et al., 1995), including peatlands (Bourgeau-Chavez et al., 2017; Hribljan et al., 2017). Because of varying moisture/flooding conditions and vegetation structure, different wetland types have been distinguished using two or more dates of L-band (~24 cm wavelength) SAR imagery alone without optical imagery (e.g. Clewley et al., 2015; Bourgeau-Chavez et al., 2013a, 2016; Whitcomb et al., 2009). Advanced Land Observation System (ALOS) Phased array–type L-band synthetic aperture radar (PALSAR) is an L-band (~24 cm wavelength) radar that orbited the earth onboard the Japanese platform from 2006 to 2011. The PALSAR sensor operated in different modes including single, dual, and quadrature polarization. The fine beam dual (FBD) polarization data of ALOS PALSAR are considered to be the most valuable for mapping on a regional basis due to their moderate resolution (20 m), 70 m × 70 m areal coverage, and two polarimetric channels—horizontal send and receive (L-HH) and horizontal send and vertical receive (L-HV). The L-HH-polarized data have been found to be most useful for detection of flooding beneath a vegetation canopy (Hess et al., 1995), while L-HV is more sensitive to differences in biomass (Bourgeau-Chavez et al., 2009). Recent wetland mapping research has demonstrated the strength of merging PALSAR and optical data for the distinction of forested, shrubby, and herbaceous wetland types (Bourgeau-Chavez et al., 2015b). Others have had success combining C-band (~5.7 cm) SAR and optical data (Dingle Robertson et al., 2015; Kloiber et al., 2015) as well as C-band SAR with LiDAR data (Millard and Richardson, 2013). Several C-band satellites have provided global data since the early 1990s (e.g., ERS, Envisat, Radarsat, Sentinel-1). This shorter wavelength is not capable of penetrating a dense forest canopy, but is useful for low stature vegetation (e.g., herbaceous vegetation, open canopy forests) and in the lowest biomass sites, is better than L-band at detecting moisture variation (Bourgeau-Chavez et al., 2013b).

While several researchers have developed methods for mapping wetlands from multisource imagery, peatlands represent a new level of detection since they typically have saturated soils but are usually not inundated and they range in vegetation cover from open to shrubby to forested. Distinguishing bogs from fens can be difficult in the field, as well as with remote sensing; however, the landscape context can aid in distinguishing bogs from fens. Further, because microwave data are sensitive to changes in moisture patterns the application of multidate imagery provides the potential to detect the differences in hydrologic patterns of bogs, which are precipitation-fed, versus fens, which are hydrologically connected to groundwater and more likely to have greater fluctuations in water table depth, moisture and inundation over time (Bourgeau-Chavez et al., 2017).

Since different peatland types have different ecological structure, it is important to use medium (10–30 m) or high (<5 m) resolution imagery to map and monitor more specific peatland types (i.e., wooded bog, open fen, etc.) and extent, and to distinguish them from the functionally different nonpeat forming wetlands (i.e., swamp, marsh, wet meadow). The choice of resolution is closely linked with the goal of the mapping effort, the size of the area to be mapped, and the timeliness and efficiency with which the map is to be produced. For regional areas, creating and updating high-resolution maps on a routine basis is generally cost and time prohibitive. Completing an area the size of boreal North America would require multiple years of effort at huge expense. Therefore, a trade-off exists between resolution and timeliness, such that timely maps can be efficiently created at a coarser resolution over the entire region, while high spatial resolution maps can generally be completed in the same timeframe for a subset of the area.

Mapping with coarse resolution imagery, such as 250 m or 1 km MODIS, leads to more generalized wetland classes and the inability to distinguish most peatlands from other wetland types. For example, Gumbricht (2012) mapped global wetlands and included a class of peat domes in the tropics but was unable to map most other peat types (note that an accuracy assessment of this map was never performed, see **Table 2**). There have been various efforts to create more detailed wetland maps for small regions of boreal Canada using aerial imagery (Vitt, 2006), LiDAR data (Chasmer et al., 2014), hyperspectral (Thomas et al., 2003), and polarimetric C-band SAR (Touzi et al., 2007). All of these focused on single date imagery. There is an effort underway to use medium resolution Landsat and C-band Radarsat data (Fournier et al., 2007; Grenier et al., 2007) for nationwide wetland mapping for the Canadian Wetland Inventory (CWI) with a minimum mapping unit of 1 ha. The CWI classification system requires mapping to five main classes (bog, fen, marsh, swamp, and shallow open water), and allows for vegetation type to be mapped in its hierarchical system, but it does not require specific distinction of open (rich) fens from treed (poor) fens or wooded bogs. A summary of boreal peatland mapping publications from the literature is provided in **Table 1** with accuracies and whether or not they distinguished peatlands. Whitcomb et al. (2009) and Clewley et al. (2015) (not listed in the table) both used two seasons of L-band data to map wetlands of Alaska with high accuracy; however, they did not distinguish peatlands from other wetland types. Grenier et al. (2007) and Li and Chen (2005) worked on developing approaches for merging Landsat and Radarsat for the CWI mapping, and Grenier et al. had 50–100% accuracy of peatland classes and 67–76% overall accuracy, while Li and Chen had 71–92% accuracy for peatland classes and 83% overall accuracy.

Dingle Robertson et al. (2015) and Millard and Richardson (2013) both used polarimetric Radarsat-2 data in combination with other sources to map peatlands with moderate success (**Table 1**). Polarimetric SAR refers to radar data that are collected in two orthogonal polarizations (generally horizontal—H and vertical—V) and the full amplitude and phase information is recorded from quadrature polarization (HH, HV, VH, and VV) send and receive polarizations. This mode fully characterizes the illuminated area on the ground and allows for more information than nonpolarimetric data. Polarimetric decompositions of the data allow for understanding the dominant scattering mechanisms and breaking down the signal into those more closely related to vegetation structure versus those more related to surface moisture/inundation. Merchant et al. used multiangle polarimetric SAR to map peatlands using support vector

**Table 1** List of reported accuracies for Boreal wetland and peatland mapping publications from the recent literature remote sensing sources and map classifiers employed

| *Publication* | *Reported accuracy* | *Input data* | *Classifier* |
|---|---|---|---|
| Whitcomb et al. (2009) | 89.5% overall peatlands not distinguished | Summer and winter JERS L-band SAR | RF |
| Grenier et al. (2007) | 67%–76% overall<br>50%–100% peatland classes | Radarsat-1 C-HH and Landsat | OBIA |
| Li and Chen (2005) | 83% overall<br>71%–92% peatland classes | Radarsat-1 C-HH and Landsat, DEM data | OBIA |
| Dingle Robertson et al. (2015) | 70% overall<br>46%–90% peatland classes | WorldView-2, DEM, polarimetric Radarsat-2 | OBIA |
| Millard and Richardson (2013) | 73% Overall<br>50%–79% peatland classes | Polarimetric Radarsat-2 and LiDAR derivatives | RF |
| Thompson et al. (2016) | 87% overall (peatland vs. nonpeatland) | National Forest Inventory k-NN dataset (forest structure data), WorldClim dataset (bioclimatic), DEM | BRT, logistic regression |
| Bourgeau-Chavez et al. (2017) | 93%, overall accuracy<br>88%–97% peatland classes | L-band PALSAR, C-band ERS, and Landsat optical-IR thermal | RF |
| Knoth et al. (2013) | 91% overall (bare peat, white birch, tussock cottongrass, sphagnum classes mapped) | UAV-based NIR | OBIA |
| Merchant et al. (2016) | 81%–84% overall<br>76%–97% peatland classes | Multiincidence angle polarimetric Radarsat-2 | SVM |

OBIA, Object based image analysis; RF, random forests; BRT, boosted regression tree; SVM, support vector machines.

**Table 2** List of reported accuracies, remote sensing sources, and map classifiers employed for tropical wetland and peatland mapping publications from the recent literature

| *Publication* | *Reported accuracy* | *Input data* | *Classifier* |
|---|---|---|---|
| Draper et al. (2014) | 64%–96% peatland classes<br>95.4% overall | Landsat, ALOS PALSAR, and SRTM | SVM |
| Hribljan et al. (2017) | 77%–96% peatland classes<br>90% overall | Multitemporal Landsat TM/PALSAR/<br>RADARSAT-1/TPI | Random forests—independent validation sites |
| Evans and Costa (2012) | 81% overall peatlands not distinguished | Multi-temporal L-band PALSAR, RADARSAT-2, and ENVISAT/ASAR | OBIA |
| Margono et al. (2014) | 89% overall compared to other maps<br>Peatlands not distinguished | Landsat, SRTM, and PALSAR | bagged classification tree model |
| Gumbricht (2012) | Not reported<br>Tropical peat domes distinguished | MODIS, MERIS (Globcover), SRTM, soils, precipitation | Spectral angle mapper |

OBIA, object based image analysis; SVM, support vector machine.

machine (SVM) algorithms with high accuracy, particularly for SAR alone as the source of input data. The multiple angles also allow for sensing different parts of the forests and vegetation as the path lengths increase with incidence angles and penetration to the ground through the canopy decreases. All of the examples in **Table 1** use state-of-the-art classifiers (OBIA, RF, BRT, and SVM).

There have been fewer peatland mapping efforts for tropical regions, particularly alpine peatlands (**Table 2**). Draper et al. (2014) used the PALSAR 50 m mosaic provided by JAXA, SRTM DEM, and Landsat data to create a map of a large portion of the Amazonia lowlands with 64–96% accuracy for the peatland classes using a SVM classifier. All of the sources were single date imagery. Margono et al. (2014) mapped Indonesia with single-date Landsat and PALSAR and DEM derivatives, but they conducted their accuracy against other wetland maps, not field data. Hribljan et al. (2017) mapped tropical alpine peatlands with high accuracy (77–96% for peatland classes) using multiseason PALSAR, Radarsat-1, and Landsat data as well as SRTM derivatives and this is described in more detail in the next section.

Note that when comparing accuracies of these maps, some of the researchers did not use independent field data sets for validation. Margono et al. (2014) compared their maps to existing wetland maps to calculate their accuracy. In addition, unless otherwise noted, those using random forests (RF) used the out-of-box accuracy provided by RF, which is biased because it is not an independent source (Bourgeau-Chavez et al., 2015b; Millard and Richardson, 2015).

## 6.04.3 Examples of Peatland Mapping in Boreal, Alpine, and Tropical Regions

In this article, we present three examples of using a combination of multidate optical and SAR imagery to map peatlands in (1) boreal Alberta, Canada; (2) alpine peatlands of Ecuador; and (3) tropical lowlands of Peru. Common to all of these examples is the use of the machine learning classifier, RF (Brieman, 2001) and two or three dates of Landsat and SAR imagery from L-band PALSAR. C-band SAR data are also used in the first two examples and SRTM DEM derivatives are used in the tropical peatland examples. RF is considered to be a state-of-the-art machine learning classifier. It is a robust method that can be applied to large areas with consistency. RF consists of multiple decision trees generated from a random subset of input training data and bands. Once the forest of decision trees is created, an individual pixel's classification is determined by which class receives the most "votes" across all decision trees. One advantage of the algorithm is that it can easily handle missing attributes, such as cloud-obscured pixels, as decision trees built without the missing attributes can be used to classify the compromised data.

In all cases, the RF approaches relied on field data for training and validation, and air photo or high-resolution satellite image interpretation using the seven elements of image interpretation (tone, texture, shape, shadow, association, size, pattern, Olson, 1960) to scale the field plots from the minimum mapping unit (0.2 ha in all cases) to create larger training polygons for input to RF. A schematic of the approach is presented in **Fig. 2**. For the first two test cases, training data were collected for each PALSAR frame and the mapped areas were divided by these frames (including Landsat data which have a larger footprint) and run through RF and mosaicked postclassification. This approach was used because the effects of rain or drying on SAR backscatter are great, therefore remote sensing training data from one frame cannot be readily used in an adjacent frame unless similar environmental conditions existed in each. However, for the third case study, lowlands of Peru, field data were limited and methods for mosaicking adjacent frames and methods to normalize the scenes to one another were necessary. Further research in using various approaches to normalizing adjacent scenes or creating super forests of field data are underway to streamline the classification process. For this third example, a preliminary map is shown in this article as research continues and additional field data are gathered.

### 6.04.3.1 Field Data Collection

Critical to all map classifications is quality field data collected at the appropriate scale (mmu) for training and validation of the maps. All field data collections should follow a protocol based on the minimum mapping unit that is related to the spatial

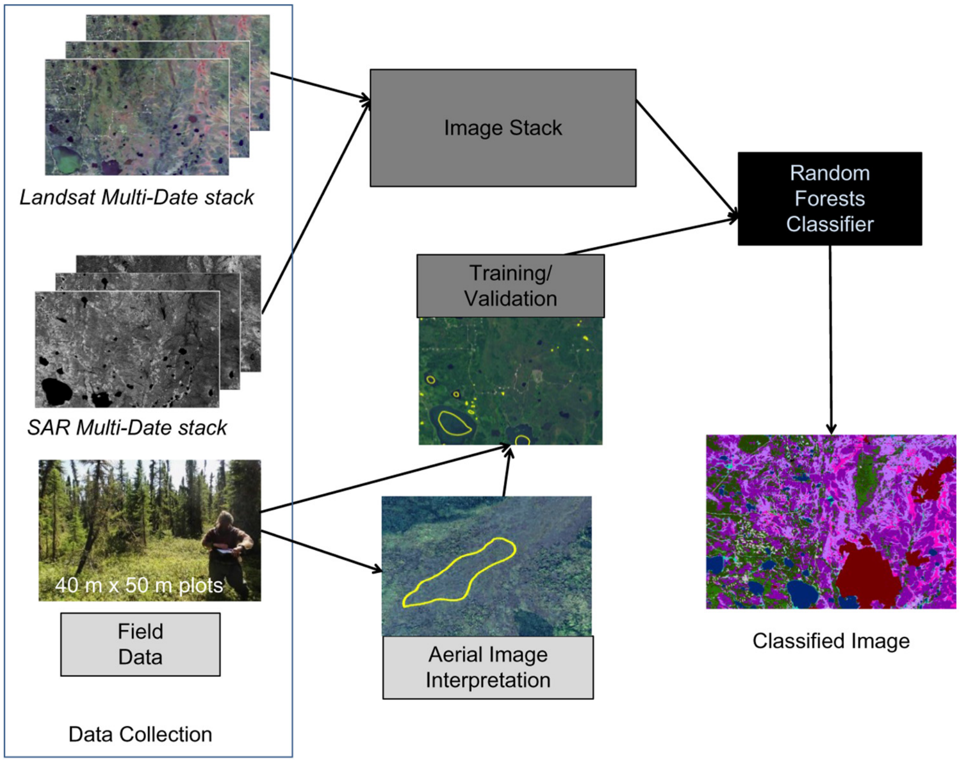


**Fig. 2** Schematic diagram showing the approach used in the article to map peatlands from a combination of SAR and optical multidate imagery using the machine learning classifier RF trained with field collected/aerial image interpreted polygon data.

resolution of the sensors. For SAR, spatial averaging and/or speckle filtering needs to be applied to correct for the inherent speckle noise. This is due to the coherent nature of the SAR systems and results in bright and dark adjacent pixels, a sort of "salt and pepper" effect. Therefore, a single pixel of SAR data cannot be used to relate to field variables, instead, a group of pixels must be averaged or otherwise filtered to reduce speckle. For medium-resolution sensors (10–20 m), we use 0.2 ha as the minimum mapping unit (mmu). This allows for $3 \times 3$ window speckle filtering of the 12.5 m pixel spacing of the SAR data ($\sim$37.5 m $\times$ 37.5 m). The corresponding field data are then collected in 40 m $\times$ 50 m plots which approximate the mmu.

The protocol for selection of sites to sample in the field consisted of systematic and/or random sampling within the regions of interest. Ideally, locations of somewhat homogeneous cover (an example of treed vs. open fen shown in Fig. 3) are randomly

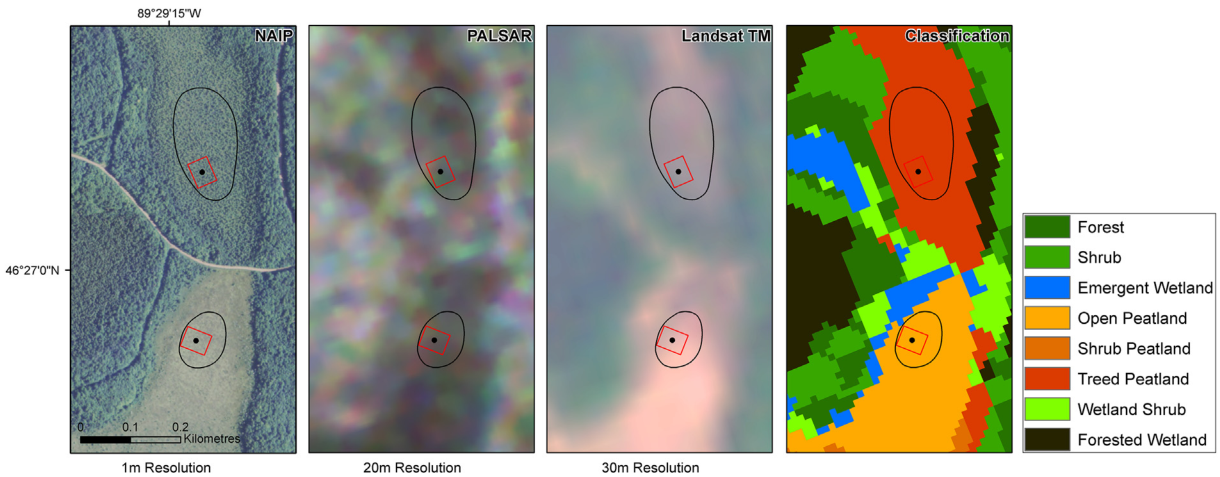


**Fig. 3** Field sampling plot (*red box*) shown in relation to the 1-m resolution aerial imagery (NAIP), 20-m resolution PALSAR, 30-m resolution Landsat, and the classified map (after Bourgeau-Chavez et al., 2017). The *red box* shows field-measured plots of 40 m $\times$ 50 m, the *black dots* are the centers of the plots. The *black-outlined polygons* are examples of air photo interpreted areas used for training the RF classifier.

sampled. However, complete random sampling may result in few actual wetland sites of interest being sampled. Therefore, a previous map of a region or quick interpretation of Google Earth imagery may help to constrain the areas sampled and then random sampling within the regions may be applied, noting that there may be constraints on distance from roads, waterways or other methods for reaching a site. For the first two example studies presented in this article, a field area such as represented by the red box of **Fig. 3** (40 × 50 m) was characterized, the black dot represents the central GPS location that would be collected along with field photos in each cardinal direction (N, S, E, and W) as well as a nadir photo. Once at a preselected field location, a homogeneous area of 0.2 ha was characterized. The field data collected in addition to photos included GPS location, characterization of the wetland type (bog, fen, marsh, swamp, upland), species diversity, dominant species composition, moisture status (inundated, soggy, moist, dry), height and density of the vegetation, and peat depth. Vegetation indicators and water chemistry can also be used in the field to aid in distinguishing bogs from fens. In addition, hand drawing of maps on the field sheet and delineations of unique vegetation types and species transition areas within wetland complexes were transcribed onto laminated aerial photographs. Included in those delineations was the larger extent of the particular cover type in the laminated aerial image of the area.

**Fig. 3** shows how the field and 1 m air photo compares to the resolution of Landsat and in this case 20 × 20 m resolution PALSAR, and finally how that looks in the final map classification conducted for peatlands of the Great Lakes (Bourgeau-Chavez et al., 2017). Field data collection at the minimum mapping unit (0.2 ha) was crucial to training the satellite data for mapping peatland classes and for validation of final products. The field data collected were used in developing training and validation polygons for classification and accuracy assessment. Navigation to each site in the remote regions of Alberta, Canada, and Ecuador was sometimes difficult, requiring traversing difficult landscapes by foot or all terrain vehicle, or by boat across rivers and lakes. Some of the data used for the Peru lowland mapping were also collected with this protocol, but because of the remoteness of this region and the logistical difficulties of field data in this region, data from other sources were also used in this mapping (e.g. Draper et al., 2014; Lähteenoja et al., 2009).

### 6.04.3.2 Training Data and Air Photo Interpretation

Training and validation polygons were interpreted by an image analyst through the use of field data and air photos to use as input to RF. Black and white infrared aerial photography was acquired in GeoTIFF format from the Alberta Environment and Sustainable Resource Development Ministry. The black and white infrared aerial photography allows for better distinction of tone and texture for peatland delineation. **Fig. 4** is an example of the photography used for delineation with polygons that were interpreted from the field data and aerial photography for Alberta Canada. Areas with smooth texture tend to be wetlands. Within the smooth texture areas, the darker toned areas tend to have more black spruce whereas the lighter regions tend to be more open. For the tropical regions, imagery available on Google Earth and WorldView-2 data were used when available. In all cases, the amount of training data created per class was proportional to the area of that class for each region. This is a necessity for RF classification (Millard and Richardson, 2015).

### 6.04.3.3 Accuracy Assessment

To create a robust validation dataset for each of the peatland type maps, training polygons which were equivalent to approximately 20% of the total polygon area of each class were withheld from the classifications and reserved for validation. Whole polygons and not partial polygons were reserved. Polygons created from field data were automatically withheld, and the remaining polygons were randomly selected. This approach was used because the out-of-box validation of RF does not represent an independent dataset for validation (Bourgeau-Chavez et al., 2015b; Millard and Richardson, 2015). The accuracy assessments included producer's accuracy, which is a measure of how accurately the analyst classified the image data (errors of omission = 100—producer's accuracy) and user's accuracy, which is a measure of how accurately a classification performed in the field (errors of commission = 100—user's accuracy) (Congalton and Green, 1999; Congalton and Green, 2008).

### 6.04.3.4 Boreal Peatland Mapping

The primary study area for developing the boreal peatland mapping approach was located in northeastern Alberta, Canada approximately 175 km north of Edmonton (**Fig. 5**). This region falls within the extensive low-lying valleys and plains of the Boreal Plains Ecozone and contains extensive peatland complexes (> 30%) intermixed with uplands. This ecozone extends from Manitoba and Saskatchewan through nearly two-thirds of Alberta (**Fig. 5** inset). The Alberta study area is permafrost-free and represents a mosaic of upland and lowland ecosystems including swamp, fen, bog, and marsh. The peatlands were dominated by black spruce (*Picea mariana*) bogs, open sedge fens and *Larix laricina* and *Picea mariana* treed fens. Hydrologic and water chemistry differences between boreal bogs, treed fens (poor), and open sedge/herb (rich) fens give rise to different plant community composition (Vitt and Chee, 1990). It is important to distinguish these different types, both fen versus bog and plant composition because the differences in hydrology and biomass result in different fire behavior and fuel consumption, which is the main threat to boreal peatlands in this region. Methods for mapping North American boreal peatlands (Bourgeau-Chavez et al., 2009, 2015b, 2017) were developed and refined using a merging of multiseason Landsat (optical/thermal) and multiseason L-band (PALSAR) and C-band (e.g. ERS) SAR data. Extensive field data were collected over a four-year period, resulting in 350 field locations (0.2 ha locations) for use as training or validation. These were supplemented with training polygons interpreted from aerial images as described above.

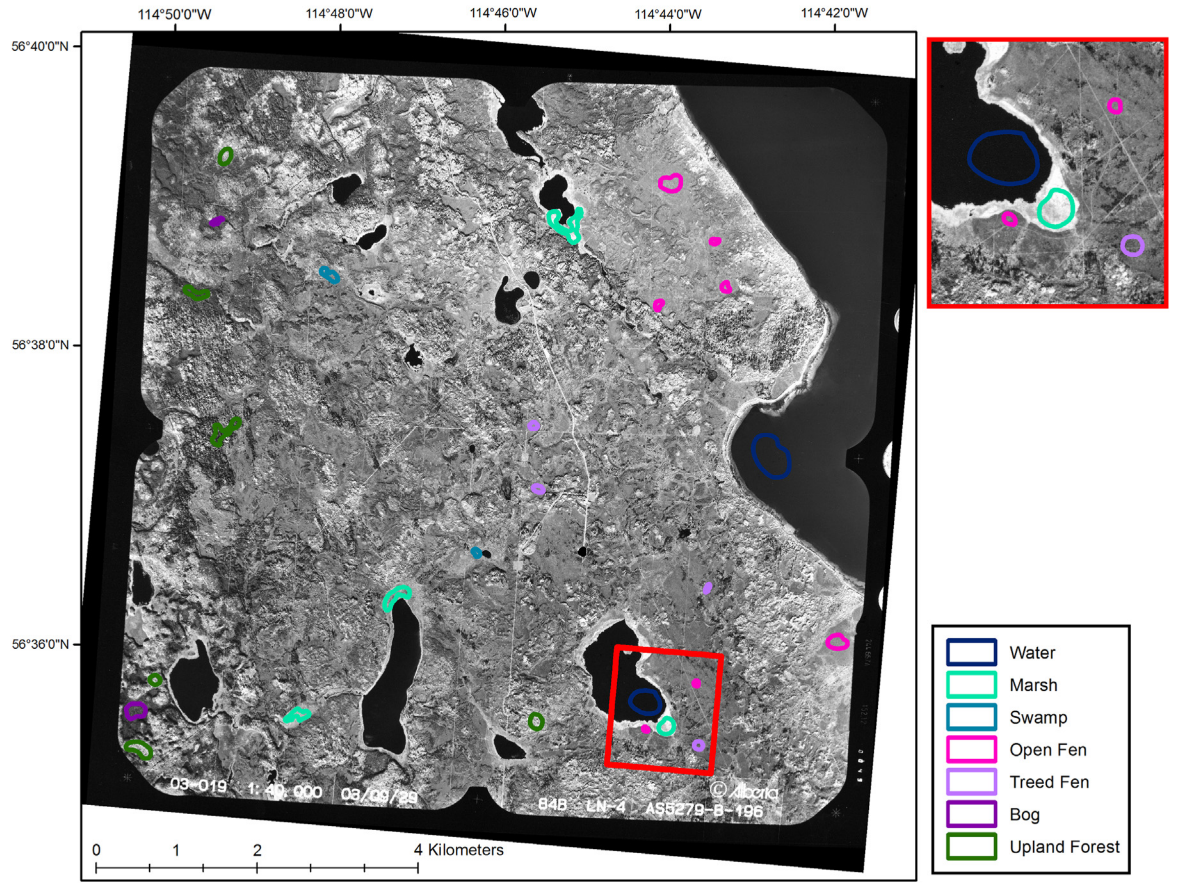


**Fig. 4** Black and white infrared aerial imagery of Alberta Canada (from the Alberta Environment and Sustainable Resource Development Ministry) was used to create training polygons of different peatland types based on field data and image interpretation.

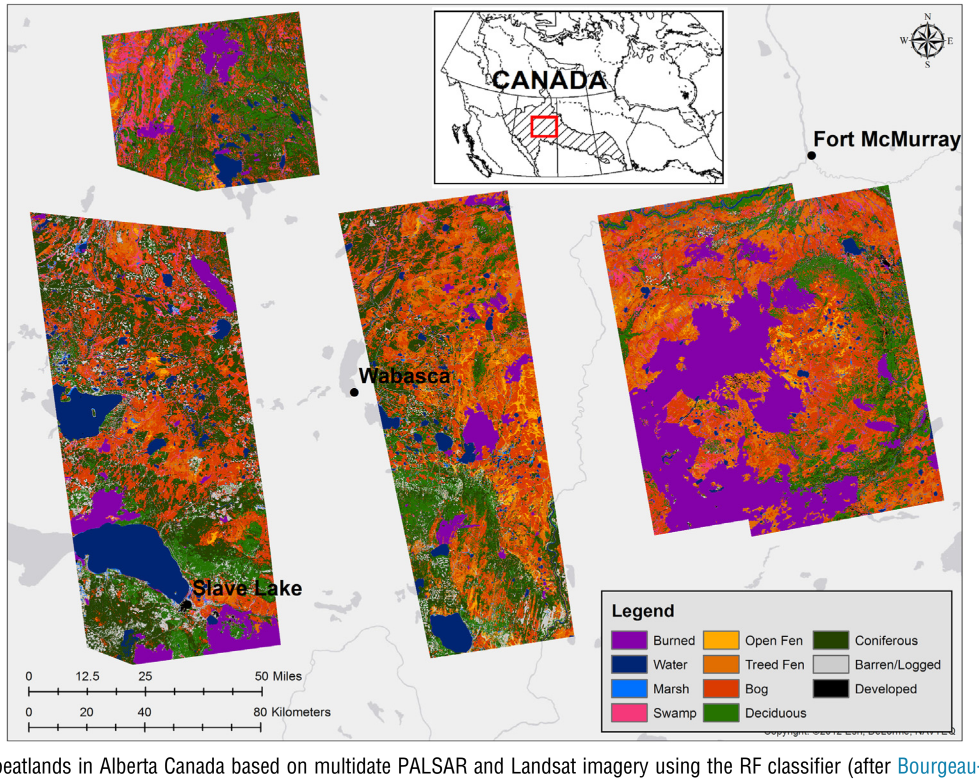


**Fig. 5** Map of peatlands in Alberta Canada based on multidate PALSAR and Landsat imagery using the RF classifier (after Bourgeau-Chavez et al., 2017). Old burned areas (preimage collection) are masked out since they are regenerating areas that were not sampled in the field or trained in RF.

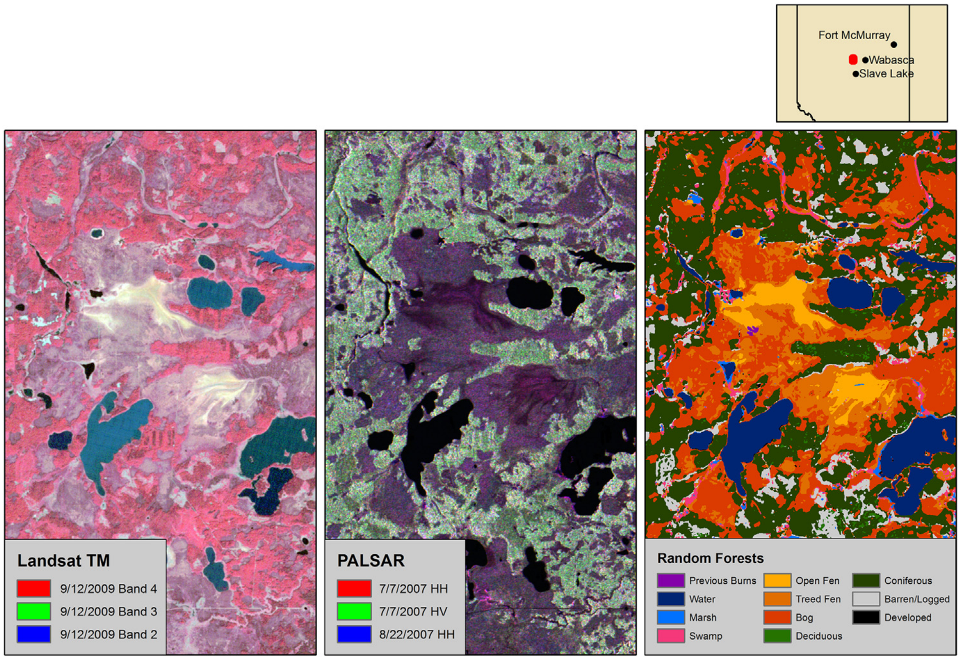


**Fig. 6** False color composite of Landsat 5 bands 4, 3, 2 from September 2009 (left); PALSAR false color composite of July 2007 HH and HV and August 2007 HH polarization (center); and the resulting RF classified map (right) of a subsetted area of the map in **Fig. 5**.

SAR HH polarization allows the differentiation of the hydrological differences between bogs and fens, while optical/thermal cross validates wet condition and aids in the differentiation of covertype along with SAR HV polarization which is sensitive to biomass (Bourgeau-Chavez et al., 2009, 2015b, 2017). A comparison of Landsat to PALSAR for a peatland-rich subarea of Alberta near Wabasca is shown in Fig. 6 along with the classified map of this area. This figure provides a look at the imagery and how bogs, treed, and open fens, as well as swamps and marshes appear in comparison to upland conifer and deciduous ecosystems.

Although Bourgeau-Chavez et al. (2017) tested several mapping algorithms (including eCognition object-based image analysis, maximum likelihood classifiers, thresholding, and RF), the machine learning (RF) classifier was found to be more efficient, consistent, and repeatable between image analysts. A schematic of the RF mapping process is presented in Fig. 2. This approach takes advantage of the field data and scaling with air photo interpretation to improve the quantity of training data for input to RF. RF was used to map four peatland-rich study regions of the Alberta Canada region with a total area of 3,384,890 ha (Fig. 5). The overall map accuracy was 93%, with all peatland classes having greater than 88% accuracy and all other classes having 75% or greater accuracy. Note that the dark-red areas are older fire scars. These areas burned before the imagery was collected and are in a state of regeneration. These were not a focus of study and were masked out. To map the regenerating types, field data would need to be collected within these various burned areas to develop appropriate training data. This will be a focus of future work.

To determine the improvement in using the multiseason and multisensor dataset, a subset of the full map (Wabasca study area Fig. 5) was employed in a comparison study. The Wabasca study area classified through RF first using a single date of Landsat Summer data only, then Summer Landsat and SAR imagery, and lastly using the full multidate Landsat and SAR dataset to determine the statistical improvement, if any, in the mapping accuracy. The results are in Table 3 which demonstrate that using the multidate data from both optical and radar sensors improves the statistical accuracy for all peatland classes with the exception of the

**Table 3** Comparison of accuracy statistics for Wabasca study area using random forests (RF) for (A) summer Landsat-only vs. (B) summer SAR-Landsat; and (C) multidate SAR-Landsat

| | *(A) Summer Landsat-only* | | *(B) Summer SAR Landsat* | | *(C) Multidate SAR Landsat* | |
|---|---|---|---|---|---|---|
| *Class* | *UA* | *PA* | *UA* | *PA* | *UA* | *PA* |
| **Water** | 100 | 100 | 100 | 100 | 100 | 100 |
| **Wooded bog** | 68 | 73 | 74 | 75 | 99 | 98 |
| **Treed fen** | 62 | 64 | 57 | 76 | 88 | 77 |
| **Open fen** | 83 | 88 | 84 | 85 | 80 | 93 |

All RF runs included the thermal channel. Terms are user's accuracy (UA) and producer's accuracy (PA). After Bourgeau-Chavez et al. (2017).

User's accuracy for open fen, which stays about the same (80–84%). User's accuracy improves for wooded bog from 68% to 99% accuracy and treed fen from 62% to 88% when multidate, multisensor data are used (**Table 3**). Similar improvements were made in producer's accuracy for the forested sites, with wooded bog improving from 73% to 98% and treed fen from 64% to 77% (**Table 3**).

This mapping approach was also applied to an area of the southernmost extent of the North American boreal forest, Michigan's Upper Peninsula (Bourgeau-Chavez et al., 2017) with 94% overall accuracy and peatland accuracy of 63–84%. In this case, the shrubby fens were being confused in some instances with the treed fens. The open fens sometimes have trees but are defined as having $<6\%$ canopy cover. Treed fens are classed with $>6$–70% trees, which is a wide range. When shrubby and treed fens are combined into a woody fen class the accuracy increases to 91% producer's accuracy and 86% user's accuracy. The peatlands of Michigan are much smaller and dominated by fens (open, shrubby and treed) with very few bogs in comparison to Alberta Canada, but Michigan's Upper Peninsula has many more swamps and marshes. Currently, peatland mapping of Northwest Territories Canada is also underway using this methodology (**Fig. 2**), in a permafrost-rich region of the taiga shield and taiga plains. This multisensor, multidate RF classification approach is thus suitable to mapping peatlands across a wide range of boreal landscapes.

The medium-resolution boreal peatland maps are allowing research to assess the vulnerability of peatlands to wild land fire. Through comparison of the spatial distribution of peat types with maps of burn severity, it has been determined that bogs are burning in Alberta with as much or more consumption than uplands in several cases. Fens are generally wetter and are burning less severely in the spring fires that are affecting northern Alberta in the 2009–2011 time frame. A long-term study of these mapped peatlands through the SAR satellite record is allowing for analysis of variations in soil moisture from the early 1990s, which shows many of them becoming drier through time, making them more susceptible to deeper burning.

### 6.04.3.5 Alpine Peatland Mapping

There has been a more limited mapping of alpine peatlands than lowland boreal and tropical peatlands. Alpine peatlands are challenging to map because they are commonly small and often intermixed with other wetland types (Eva et al., 2004; Anaya et al., 2015). Furthermore, some mountain ranges have persistent cloud cover making it difficult to obtain cloud-free images (Anaya et al., 2015). In addition, nonpeatland areas can be floristically similar to the peatlands and are hence hard to differentiate when only using optical sensors. SAR data can be beneficial to alpine peatland mapping because of the ability to detect moisture and biomass variations. Some Alpine areas, including the páramo study area, are also challenging for SAR because the nonpeatland areas are also wet most of the year. A multisensor SAR-optical approach had not yet been applied to alpine peatlands, in part because of the complex topography of most alpine landscapes which can cause excessive distortions of the SAR signals (e.g., layover, fore-shortening) and must be corrected (Atwood et al., 2014). The multidate, multisensor SAR and optical approach shown to be useful in boreal peatlands by Bourgeau-Chavez et al. (2017) was therefore applied to the páramo region of the Andes in northeastern Ecuador to test its suitability (Hribljan et al., 2017).

The páramo contains a diverse range of ecosystem types including extensive well-drained grasslands, scrubland, high Andean forests, and peatlands (Hofstede et al., 2003). Three distinct types of peatlands were identified in this region; cushion, grass, and sedge peatlands. Cushion peatlands are poorly drained areas clearly dominated by the conspicuous cushion and matt-forming species (*Distichia* spp., *Plantago rigida*, *Disterigma empetrifolium*, *Oreobolus ecuadoriensis*). Cushion plants are usually $<10$ cm tall. Grass peatlands are poorly drained areas structurally dominated by a matrix of grasses (*Cortaderia sericantha*, *C. nitida*, *Festuca* spp.), a sparse layer of shrubs (e.g., *Loricaria* sp., and *Hypericum lancioides*) and a rich herb layer (e.g., *Niphogeton* sp., *Huperzia* spp., *Gunnera maguellanica* and *Hypochaeris* spp.). Sedge peatlands are poorly drained areas dominated by a dense matrix of several species of Cyperaceae (e.g., *Carex* spp., *Uncinia*, spp. *Eleocharis* spp.) and a sparse layer of herbs and mosses might be present (e.g., *Niphogeton* sp., *Gunnera maguellanica*). Extensive field surveys aided in estimating mountain peatland spatial extent in this challenging alpine environment. The field data collection resulted in 91 field sites including 22 cushion peatlands, 41 grass peatlands, 10 sedge peatlands, and 28 upland sites. High resolution satellite imagery (e.g. Worldview-2) was used to expand these field data to create additional training data through image interpretation.

Since the páramo was dominated by nontreed peatlands, two different wavelengths of SAR data were used: L-band from ALOS PALSAR and C-band from RADARSAT-1. The shorter wavelength of C-band ($\sim 5.7$ cm) has been found as more suitable to detect changes in moisture in low stature vegetated sites (Bourgeau-Chavez et al., 2013b). In addition, optical imagery combined with digital elevation model (DEM) data were used. Landsat data provide information on vegetation type and wetness to some degree in these low-stature vegetated systems and SAR provides information on hydrological characteristics of wetlands and vegetation structure. Due to the large topographic variation in the study area, it was important to include DEM data for accurate terrain correction of the imagery and for topographic analysis. We used SRTM data filled with ASTER DEM data. In addition, a topographic position index (TPI), derived from the DEM data, was included to inform the classifier about landform and slope position, identifying low-lying conditions suitable for peat development. Using multiple dates of imagery allows the capture of phenological differences between plant species and differences in hydrology among seasons, further improving peatland differentiation. The multisource multidate map is presented in **Fig. 7**. To determine the importance of the different input data sources a comparison of different band combinations was completed. The RF classifier was run with the same supervised training data set and in all cases multidate data to evaluate the performance of (1) Landsat alone; (2) Landsat and TPI; (3) Landsat and Radarsat; (4) Landsat, Radarsat and TPI; (5) Landsat/PALSAR/Radarsat and TPI; and (6) PALSAR Radarsat, and TPI. This allowed for comparing SAR only, in this often cloud-covered environment, and Landsat-only, which is often used alone in map applications, as well as combinations of the data sources.

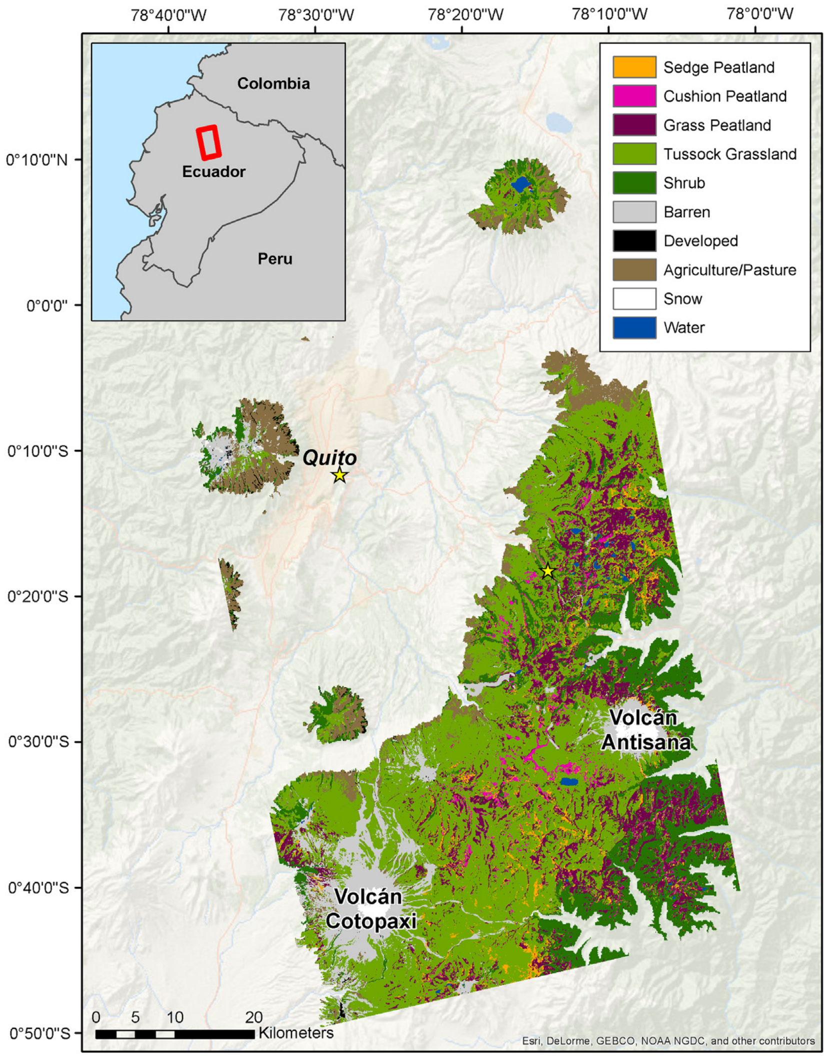


**Fig. 7** Ecuador alpine peatland map of a 5500 km$^2$ study area based on multidate, multisensor Landsat, PALSAR, Radarsat-1, and TPI (after Hribljan et al. 2017). Mapping area below 3500 masl is grayed out. Upper left inset shows the mapped area location.

Results of the statistical comparison of the different data sources showed that using PALSAR/Radarsat/TPI (Fig. 8) without optical data had less than desirable results, with only 61% overall accuracy and low peatland class accuracies ranging from 48% to 81%. This was disappointing because it would be useful to be able to use SAR from multiple dates and sources in this often cloud-covered location. Polarimetric SAR may provide improvements as described earlier, and they should be evaluated. Next, the Landsat-only map had a fairly high overall accuracy of 86%; however, there was a moderate error in distinguishing between the peatland classes (Table 4, Fig. 8). Adding multidate Radarsat into the classifier (Table 4, Fig. 8) slightly improved the overall accuracy (87%), especially for grass peatlands. There was, however, a slight drop in cushion peatland accuracy. When TPI was also used in the mapping (Table 4), overall accuracy remained the same, but there was a further improvement in the user's accuracy for all peatland classes, as well as an increase in producer's accuracy for grass peatland. The producer's accuracy for sedge and cushion peatland dropped slightly. When Landsat/Radarsat/PALSAR/TPI (Table 4, Fig. 8) were used together, the overall accuracy was the greatest at 90%, and the individual peatland class accuracies increased or stayed the same for all classes except the producer's accuracy for cushion peatland, which decreased slightly to 80%.

In comparing the different input data sources for mapping, it is important to also look at the maps themselves and not just review the statistics on accuracy. Fig. 8 shows a comparison of the map from Landsat alone, Landsat and Radarsat, SAR and TPI (Radarsat, PALSAR, and TPI) and the multidate, multisensor Landsat, Radarsat, PALSAR, and TPI. While the overall accuracy of all but the SAR-TPI classification had 86–90% accuracy, the map products vary. Landsat is a workhorse in mapping landcover, but in distinguishing wetlands and peatlands it falls short. Although the Landsat-only map (Fig. 7) does a great job at distinguishing many of the upland classes, it greatly overestimates a number of peatlands, especially the sedge peatland class, probably due to the fact that the vegetation in the nonpeatland shrubby and open areas was quite similar to the peatland vegetation. In contrast, the SAR/TPI map was underestimating the area of peatland in much of the map, likely because the hydrology of the nonpeatlands

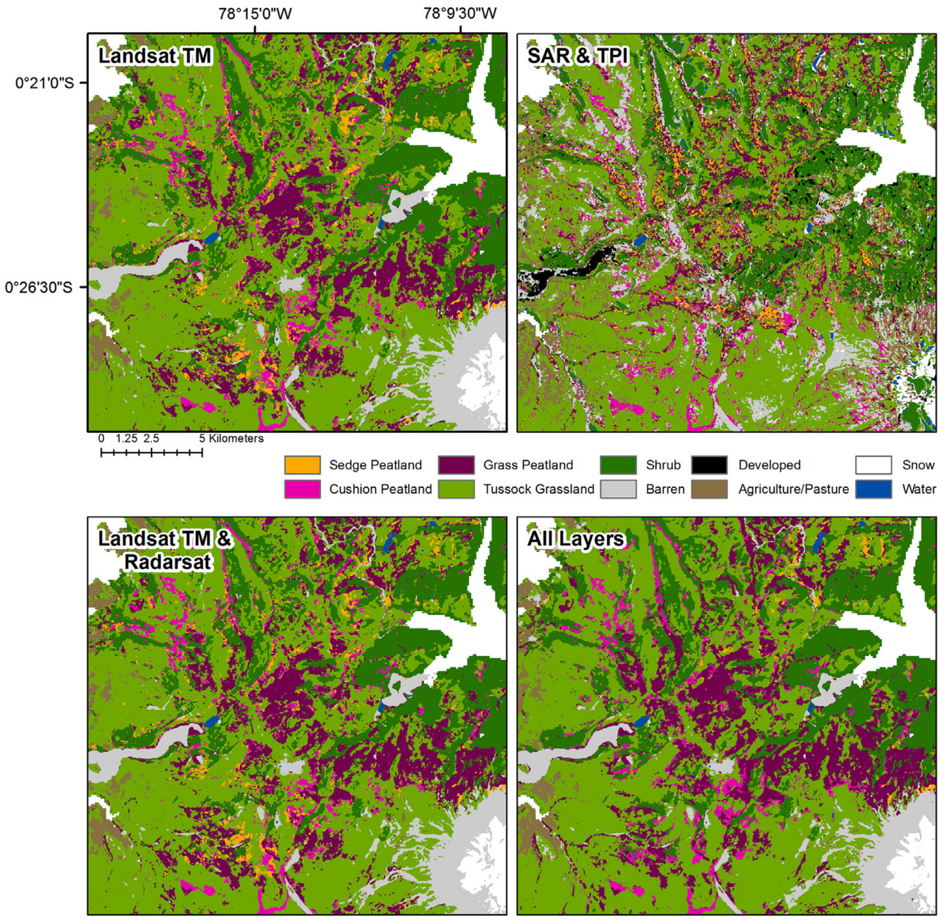


**Fig. 8** Comparison of random forests classified maps using Landsat (top left); SAR (PALSAR and Radarsat-1) and TPI (top right); Landsat and Radarsat-1 (bottom left); and all layers (Landsat, Radarsat, PALSAR, and TPI, after Hribljan et al., 2017). Multidate data were used in all cases to create the classified maps.

**Table 4** Comparison of user's accuracy (UA) and producer's accuracy (PA) for peatland classes of five different RF classifications of the paramo of Ecuador using Landsat; Landsat and Radarsat; Landsat, Radarsat, and TPI; Landsat, Radarsat, PALSAR, and TPI; and PALSAR, Radarsat, and TPI

| | *Landsat only* | | *Landsat-Radarsat* | | *Landsat-Radarsat-TPI* | | *Landsat-Radarsat-PALSAR-TPI* | | *PALSAR-Radarsat-TPI* | |
|---|---|---|---|---|---|---|---|---|---|---|
| *Class* | *UA (%)* | *PA (%)* | *UA (%)* | *PA (%)* | *UA (%)* | *PA (%)* | *UA (%)* | *PA (%)* | *UA (%)* | *PA (%)* |
| **Sedge peatland** | 89 | 81 | 92 | 86 | 94 | 83 | 94 | 86 | 70 | 54 |
| **Cushion peatland** | 93 | 85 | 92 | 83 | 93 | 81 | 95 | 80 | 81 | 55 |
| **Grass peatland** | 68 | 87 | 72 | 90 | 74 | 93 | 77 | 96 | 54 | 48 |
| **Overall accuracy** | 86 | | 87 | | 87 | | 90 | | 61 | |

After Hribjlan et al. (2017).

is also sometimes wet and thus difficult to distinguish with SAR alone and it often falls short without the aid of optical imagery to detect the vegetation type differences. While in other areas the SAR/TPI was overestimating the peatland area (e.g. in the steepest terrain), it is the synergy of the SAR (which is sensing backscatter differences due to hydrology) and Landsat (that is sensing the vegetation types) that allows for an improved distinction of peatland types. The C-band Radarsat HH polarization imagery was of higher importance than PALSAR for distinguishing the peatland types, but adding the L-band PALSAR data (HH and HV) into the classification refined the accuracy of nearly all of the map classes (Table 4).

The multidate Landsat/Radarsat/PALSAR/TPI map had an overall accuracy of 90%. This map shows 48,218 ha of peatland, which represents 17.8% of our páramo study area. Overall, the accuracy of this method for distinguishing peatlands from nonpeatlands was very high: the combined peatland classes in this map had user's and producer's accuracy of 95%. This was so high because many of the classification errors were among peatland vegetation classes.

#### *6.04.3.5.1 Peatland coverage in the Ecuadorian Páramo*

This multidate, multisensor map (Fig. 6) provides the first estimate of regional peatland coverage and combined with field sampling of peat cores, C storage in the Andean páramo. We detected 482 $km^2$ of peatlands across our mapping region, an increase of $\sim 3.4\times$ and $23.7\times$ over the previous mapping efforts of Beltrán et al. (2009) and the Ecuadorian Ministry of the Environment (MAE) (http://mapainteractivo.ambiente.gob.ec/), respectively. Our results highlight peatlands as an important feature of the high-altitude páramo environment. Moreover, the current mapping products are the only products available in Ecuador to inform environmental policy and ecosystem management. This is a critical concern for Ecuadorian land managers that are in need of high-quality baseline mapping data to define sustainable land use practices and prioritize restoration activities in the rapidly changing páramo landscape.

### 6.04.3.6 Tropical Lowland Peatland Mapping

The final case study presented focuses on a very large remote peatland complex in Amazonia Peru covering 176,000 $km^2$ and spanning 68 PALSAR scenes. This region is very remote and difficult to access and, currently, there are limited field data available. The landscape is a mosaic of uplands and wetlands, both peat forming (open peatland that is dominated by herbs, palm swamps, and pole forest peatlands) and nonpeat forming (seasonally flooded forest and occasionally flooded forest). Through synthesis of field data from multiple sources, a total of 359 field locations were compiled and grouped into like classes. The field data were located primarily in the eastern part of the study area along roads and rivers. Many of the points consisted of transect data with multiple points in one complex. These points were grouped to form single training polygons which further reduced the number of field training locations. Since the field data are not distributed equally across the study area, mapping by PALSAR scene as was done in the previous two examples would be impossible. Therefore, new mosaicking methods were tested for classifying peatlands in this large area with limited field data. These methods included matching images from similar seasons/moisture conditions and using principal component analysis (PCA) to find the dominant features.

In addition, precipitation data were used to select a set of wet and dry season images from the PALSAR database for creating two mosaics, one for each season. The same years and similar dates were chosen when possible and then dates with similar moisture were mosaicked for each season (wet and dry). A PCA was also used based on the input of all available temporal PALSAR data ($\sim 10$ dates per scene). PCA is a multivariate statistical technique to identify dominant spatial and temporal backscatter signatures. We found band one to be useful in identifying consistent patterns across scenes, and this was used along with the mosaicks of wet and dry season data in the RF layer stack. Cloud-free Landsat was very limited for this area and similar dates were not available across the study area. We, therefore, used the circa 2000 Landsat 7 cloud-free composite created by Hansen et al. (2013) for Peru. Another Landsat composite existed for circa 2014 but it was abandoned due to the striping over the study area (Landsat 7). The cloud-free 2000 image composite included Landsat bands 3 (red), 4 (NIR), 5 (SWIR), and 7 (SWIR).

In this lowland tropical area, peatland doming occurs so DEM data were also included to try to capture these features. A TPI was derived from the SRTM to help differentiate peatland doming from uplands.

The preliminary map (Fig. 9) had high individual class accuracy, especially for peatlands (78–99% accuracy) and the map had an overall accuracy of 93%. A comparison of this map based on single-date Landsat, dry season PALSAR, wet season PALSAR, PALSAR PC1, and SRTM TPI was made to the layers used by Draper et al. (2014) which included one date of Landsat, SRTM and one date of PALSAR (which appears to be from the dry season, but is not reported). The map using the Draper remote sensing layers in RF had a similar accuracy table to what was reported in the 2014 article (64–96% accuracy for peatland classes—note that Draper used SVM, not RF). In comparison, the multidate SAR-optical-DEM map showed improvement in statistical accuracy for many of the peatland classes. Since the multidate SAR-optical-DEM approach included a wet season PALSAR mosaic, it appears to pick up much more seasonally flooded forests (light green of Fig. 9), which may be inaccurate. This map is preliminary and work continues to improve it through additional field training data and removal of inappropriate training data (such as polygons that straddle two or more classes). Millard and Richardson (2015) found a selection of training data and input variables to have a strong influence on the overall accuracy of RF classification. It is important to have the proportion of training data mimic the proportion on the landscape for RF since it is highly sensitive to the size of the training dataset (Millard and Richardson, 2015). This is difficult to accomplish in such a remote location where most of the field data were collected in a small portion of the map area. This preliminary map is currently under review by the team, including regional experts who have a great deal of experience on the landscape. This is an important step in developing an accurate map, because statistics may show the map as highly accurate, but it may not be representative of the landscape as a whole.

## 6.04.4 Summary and Future Research

Peatlands are just one of many ecosystems experiencing a rapidly changing environment. Changes to peatlands occur as a result of both anthropogenic (e.g., agriculture conversion, drainage, mining) and climatic (e.g., permafrost thaw, increased fire intensity and frequency) effects. While these changes unfold remote sensing offers the ability to monitor these changes at broad scales and capture the resulting impacts.

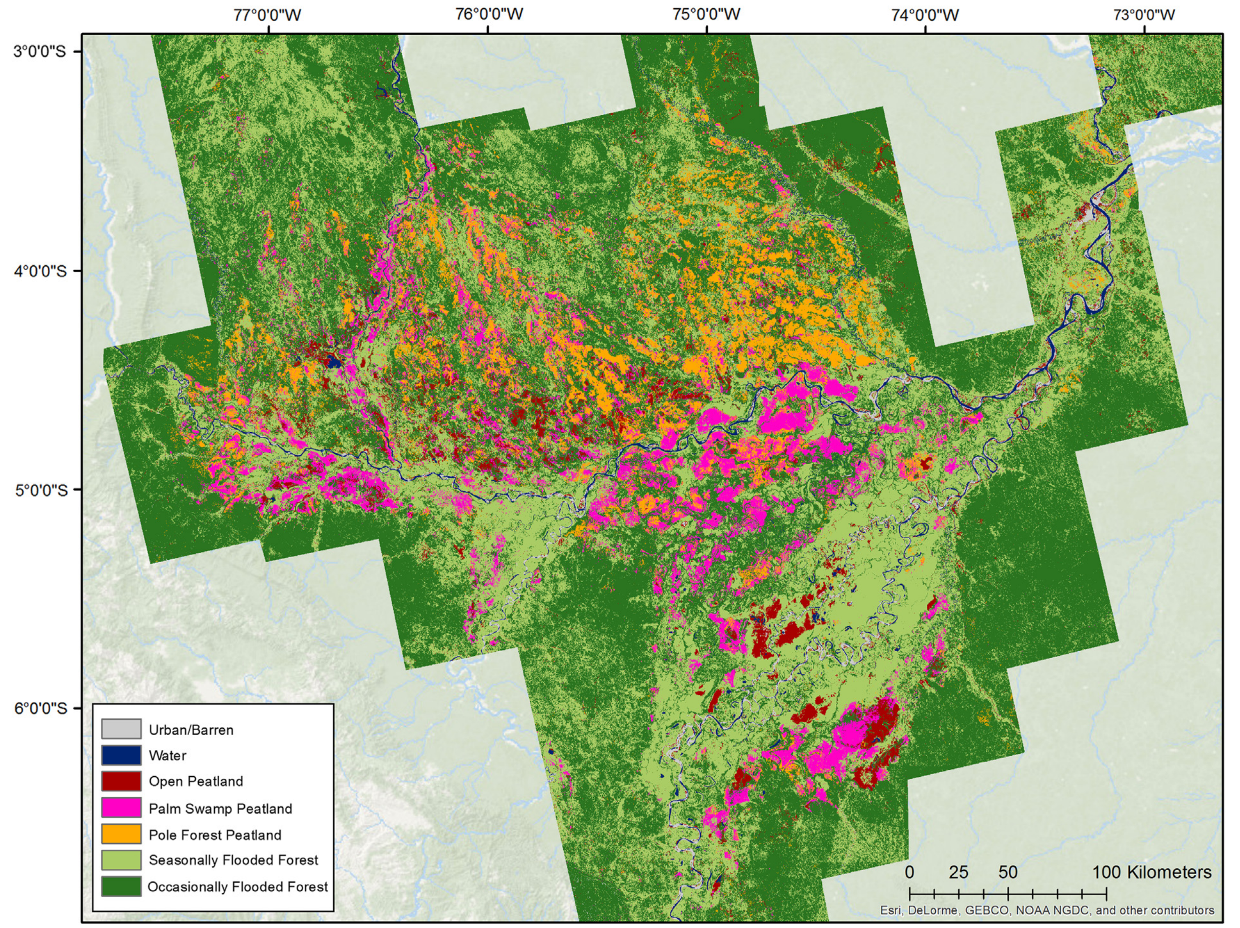


**Fig. 9** Lowland Peruvian Amazon preliminary peatland map based on multidate PALSAR, Landsat, and SRTM. Refinement of this map is underway with further assessment by regional experts and collection of additional field data for training.

**Table 5** Accuracy assessment for the tropical lowland map of Peru peatlands created from multidate PALSAR, SRTM, and one date of Landsat

| | *Reference ground truth classes* | | | | | | | | | |
|---|---|---|---|---|---|---|---|---|---|---|
| *Mapped classes* | *Urban/ barren* | *Water* | *Open peatland* | *Palm swamp peatland* | *Pole forest peatland* | *Seasonally flooded forest* | *Occasionally flooded forest* | *Sum* | *Commission error (%)* | *User Acc. (%)* |
| **Urban/barren** | 208 | 0 | 0 | 0 | 0 | 0 | 0 | 208 | 0 | 100 |
| **Water** | 0 | 199 | 0 | 0 | 0 | 0 | 0 | 199 | 0 | 100 |
| **Open peatland** | 3 | 0 | 191 | 15 | 0 | 0 | 0 | 209 | 8.6 | 91.4 |
| **Palm swamp peatland** | 0 | 0 | 0 | 158 | 1 | 4 | 0 | 163 | 3.1 | 96.9 |
| **Pole forest peatland** | 0 | 0 | 3 | 5 | 205 | 28 | 3 | 244 | 16 | 84 |
| **Seasonally flooded forest** | 1 | 0 | 0 | 8 | 0 | 165 | 2 | 176 | 6.2 | 93.8 |
| **Occasionally flooded forest** | 0 | 0 | 12 | 16 | 0 | 5 | 197 | 230 | 14.3 | 85.7 |
| **Sum** | 212 | 199 | 206 | 202 | 206 | 202 | 202 | | | |
| **Omission (%)** | 1.9 | 0 | 7.3 | 21.8 | 1.5 | 18.3 | 2.5 | | | |
| **Prod. Acc. (%)** | 98.1 | 100 | 92.7 | 78.2 | 99.5 | 81.7 | 97.5 | | | |

Overall accuracy is 93%.

Effective use of remote sensing for any environmental application requires an understanding of both the sensor's characteristics and interactions between the sensor and the environment, a relationship not to be understated, especially when mapping peatlands. To accurately map peatlands, generally, more information about the landform, vegetation types (and seasonal phenology), vegetation structure, ground moisture and inundation (seasonal hydrology) provides improved mapping capability rather than relying on a single source of remote sensing data. The combination of one or more sensors for detection and mapping of land cover classes has been suggested as a technique to improve map accuracy by allowing for a range of characteristics to be detected (Henderson and Lewis, 2008) and several researchers have explored such techniques for mapping peatlands as has been described in this article.

The application of remote sensing to mapping and monitoring peatlands includes quantifying the loss of peatland area to palm plantations in the tropics (Koh et al., 2011), calculating rates of deforestation in Southeast Asia (Miettinen et al., 2011), and land use change in Malaysia (Miettinen et al., 2016). In the boreal zones remote sensing has been used to map permafrost thaw (Beilman and Robinson, 2003), model NPP in Saskatchewan (Kimball et al., 2000), predict surface hydrology in *Sphagnum*-dominated peatlands (Harris and Bryant, 2009), classifying peatlands in Canada (e.g. Bourgeau-Chavez et al., 2017; Millard and Richardson, 2013), monitoring organic layer soil moisture in peatlands (Bourgeau-Chavez et al., 2017b) and mapping fire severity in peatlands from Landsat (Bourgeau-Chavez, 2014). Analyses of these types help estimate not just total carbon storage, but also rates of C gain or loss as a result of disturbance over time.

There are numerous problems associated with accurate estimation of the extent of peatlands, which include a lack of standardized definition of peat depth and soil properties to be considered a peatland (30–50 cm depth); the inaccessibility of many areas to conduct required ground surveys; differences in methodology for delineating peatlands, for both on the ground techniques and remote sensing; and ongoing land use change that results in the loss of peatland area (Page et al., 2006). Improved delineation of peatland types from remote sensing ameliorate some of these problems and lead to improved estimates of peatland carbon stocks in global models (e.g. Yu et al., 2010). A variety of methods have been developed in an attempt to map with higher accuracy at medium spatial resolution or with greater efficiency at a finer resolution. Advances in sensing instruments and image processing software have allowed significant improvement in mapping capability, efficiency, and accuracy as has been summarized in this article. In addition to the state-of-the-art classifiers used in many recent mapping efforts, new investigation into Deep Learning algorithms and using UAVs for assessing field characteristics (training and validation) in these remote peatland areas should improve the mapping of peatlands in both tropical and boreal environments.

*See also:* 1.07. The EUMETSAT Polar System. 9.19. Remote Sensing Data and Methods for Identifying Urban and Peri-Urban Smallholder Agriculture in Developing Countries and in the United States.

## References

Anaya, J. A., Colditz, R. R., & Valencia, G. M. (2015). Land cover mapping of a tropical region by integrating multi-year data into an annual time series. *Remote Sensing, 7*(12), 16274–16292.

Anderson, J. A. R. (1983). The tropical peat swamps of western Malaysia. In *Mires: Swamp, bog, fen and moor: Regional studies*. Amsterdam: Elsevier.

Atwood, D. K., Andersen, H. E., Matthiss, B., & Holecz, F. (2014). Impact of topographic correction on estimation of aboveground boreal biomass using multi-temporal, L-band backscatter. *IEEE Journal of Selected Topics in Applied Earth Observations and Remote Sensing, 7*(8), 3262–3273.

Bauer, I. E., Gignac, L. D., & Vitt, D. H. (2003). Development of a peatland complex in boreal western Canada: Lateral site expansion and local variability in vegetation succession and long-term peat accumulation. *Canadian Journal of Botany, 81*(8), 833–847.

Beilman, D. W., & Robinson, S. D. (2003). Peatland permafrost thaw and landform type along a climatic gradient. In , *1*. In: *Proceedings of the 8th International Conference on Permafrost* (pp. 61–65). Zurich: Balkema.

Beltrán K, Salgado S, Cuesta F, León-Yánez S, Romoleroux K, Ortiz E, Cárdenas A, Velástegui A (2009) *Distribución espacial, sistemas ecológicos y caracterización florística de los páramos en el Ecuador*. EcoCiencia, Proyecto Páramo Andino y Herbario QCA. Quito, Ecuador.

Benavides, J. C., Vitt, D. H., & Wieder, R. K. (2013). The influence of climate change on recent peat accumulation patterns of Distichia muscoides cushion bogs in the high-elevation tropical Andes of Colombia. *Journal of Geophysical Research: Biogeosciences, 118*(4), 1627–1635.

Botch, M. S., Kobak, K. I., Vinson, T. S., & Kolchugina, T. P. (1995). Carbon pools and accumulation in peatlands of the former Soviet Union. *Global Biogeochemical Cycles, 9*(1), 37–46.

Bourgeau-Chavez, L. L. (2014). *Final Report to NASA on Grant # NNX09AM15G entitled "Vulnerability of North American Peatlands to Interactions between Climate, Hydrology and Wildland Fires"*.

Bourgeau-Chavez, L., Endres, S., Banda, E., Powell, R. B., Turetsky, M., Benscoter, B. W., & Kasischke, E. (2015a). *NACP peatland landcover type and wildfire burn severity maps, Alberta, Canada*. Tennessee: ORNL DAAC, Oak Ridge.

Bourgeau-Chavez, L., Endres, S., Battaglia, M., Miller, M., Banda, E., Laubach, Z., Higman, P., Chow-Fraser, P., & Marcaccio, J. (2015b). Development of a bi-national great lakes coastal wetland and land use map using three-season PALSAR and Landsat imagery. *Remote Sensing, 7*(7), 8655. http://dx.doi.org/10.3390/rs70708655.

Bourgeau-Chavez, L. L., Endres, S., Powell, R., Battaglia, M. J., Benscoter, B., Turetsky, M., Kasischke, E. S., & Banda, E. (2017). Mapping boreal peatland ecosystem types from multi-temporal radar and optical satellite imagery. *Canadian Journal of Forest Research, 47*(4), 545–559. http://dx.doi.org/10.1139/cjfr-2016-0192.

Bourgeau-Chavez LL, French NHF, Graham JA, Kleiman S, Miller ME, Billmire M, and Jenkins L (2017b) Estimating burn severity in boreal peatlands due to wildfire from Landsat imagery. *International Journal of Wildland Fire*. (in prep).

Bourgeau-Chavez, L. L., Kowalski, K. P., Mazur, M. L. C., Scarbrough, K. A., Powell, R. B., Brooks, C. N., Huberty, B., Jenkins, L. K., Banda, E. C., Galbraith, D. M., Laubach, Z., & Riordan, K. D. (2013a). Mapping invasive Phragmites australis in the coastal Great Lakes with ALOS PALSAR satellite imagery for decision support. *Journal of Great Lakes Research Supplement, 39*, 65–77. http://dx.doi.org/10.1016/j.jglr.2012.11.001.

Bourgeau-Chavez, L. L., Leblon, B., Charbonneau, F., & Buckley, J. R. (2013b). Evaluation of polarimetric Radarsat-2 SAR Data for development of soil moisture retrieval algorithms over a chronosequence of black spruce boreal forests. *Remote Sensing of Environment, 132*, 71–85. http://dx.doi.org/10.1016/j.rse.2013.01.006.

Bourgeau-Chavez, L., Lee, Y. M., Battaglia, M., Endres, S. L., Laubach, Z. M., & Scarbrough, K. (2016). Identification of woodland vernal pools with seasonal change PALSAR data for habitat conservation. *Remote Sensing, 8*(6), 490. http://dx.doi.org/10.3390/rs8060490.

Bourgeau-Chavez, L. L., Riordan, K., Powell, R. B., Miller, N., & Nowels, M. (2009). Improving wetland characterization with multi-sensor, multi-temporal SAR and optical/infrared data fusion. In *Advances in Geoscience and Remote Sensing*. Croatia, Rijeka: InTech.

Bridgham, S. A., Updegraff, K., & Pastor, J. (1996). Carbon, nitrogen and phosphorus mineralization in northern wetlands. *Ecology, 79*, 1545–1561.

Brieman, L. (2001). Random Forests. *Machine Learning, 45*(1), 5–32.

Calmé, S., & Desrochers, A. (2000). Biogeographic aspects of the distribution of bird species breeding in Québec's peatlands. *Journal of Biogeography, 27*(3), 725–732.

Chapin, F. S., McGuire, A. D., Randerson, J., Pielke, R., Baldocchi, D., Hobbie, S. E., Roulet, N., Eugster, W., Kasischke, E., Rastetter, E. B., & Zimov, S. A. (2000). Arctic and boreal ecosystems of western North America as components of the climate system. *Global Change Biology, 6*(S1), 211–223.

Charman, D. (2002). *Peatlands and environmental change*. Chichester: John Wiley and Sons LTD.

Charman, D. J., Hohl, V., Beilman, D. W., Blaauw, M., Booth, R. K., Yu, Z. C., Loisel, J., Brewer, S., Chambers, F. M., Christen, J. A., & Gallego-Sala, A. (2013). Climate-related changes in peatland carbon accumulation during the last millennium. *Biogeosciences, 10*(2), 929–944.

Chasmer, L., Hopkinson, C., Veness, T., Quinton, W., & Baltzer, J. (2014). A decision-tree classification for low-lying complex land cover types within the zone of discontinuous permafrost. *Remote Sensing of Environment, 143*, 73–84.

Chimner, R. A. (2004). Soil respiration rates in tropical peatlands of Micronesia and Hawaii. *Wetlands, 24*, 51–56.

Chimner, R. A., & Ewel, K. C. (2005). A tropical freshwater wetland: II. Production, decomposition, and peat formation. *Wetlands Ecology and Management, 13*(6), 671–684.

Chimner, R. A., & Karberg, J. M. (2008). Long-term carbon accumulation in two tropical mountain peatlands, Andes Mountains, Ecuador. *Mires and Peat, 3*(4), 1–10.

Chimner, R. A., Cooper, D. J., & Lemly, J. M. (2010). Mountain fen distribution, types and restoration priorities, San Juan Mountains, Colorado, USA. *Wetlands, 30*, 763–771.

Chimner, R. A., Ott, C. A., Perry, C. H., & Kolka, R. K. (2014). Developing and evaluating rapid field methods to estimate peat carbon. *Wetlands, 34*(6), 1241–1246.

Clewley, D., Whitcomb, J., Moghaddam, M., & McDonald, K. (2015). Chapter 17: Mapping the state and dynamics of boreal wetlands using synthetic aperture radar. In R. Tiner, M. Lang, & V. Klemas (Eds.), *Remote sensing of wetlands: Applications and advances* (pp. 369–398). Boca Raton: CRC Press.

Clymo, R., Turunen, J., & Tolonen, K. (1998). Carbon accumulation in peatland. *Oikos, 81*(2), 368–388. http://dx.doi.org/10.2307/3547057.

Cochrane, M. A. (2003). Fire science for rainforests. *Nature, 421*(6926), 913–919.

Congalton, R. G., & Green, K. (1999). *Assessing the accuracy of remotely sensed data: principles and practices*. Boca Raton, Fl, USA: Lewis Publishers.

Congalton, R. G., & Green, K. (2008). *Assessing the accuracy of remotely sensed data: principles and practices*. Boca Raton, Fl, USA: CRC press.

Cooper, D. J., Chimner, R. A., & Merrit, D. M. (2012). *Western mountain peatlands*. Berkeley, CA, USA: University of California Press.

Dargie, G. C., Lewis, S. L., Lawson, I. T., Mitchard, E. T. A., Page, S. E., Bocko, Y. E., & Ifo, S. A. (2017). Age, extent and carbon storage of the central Congo Basin peatland complex. *Nature, 542*(7639), 86–90.

Dingle Robertson, L., King, D. J., & Davies, C. (2015). Object-based image analysis of optical and radar variables for wetland evaluation. *International Journal of Remote Sensing, 36*(23), 5811–5841.

Donato, D. C., Kauffman, J. B., Murdiyarso, D., Kurnianto, S., Stidham, M., & Kanninen, M. (2011). Mangroves among the most carbon-rich forests in the tropics. *Nature Geoscience, 4*(5), 293–297.

Dorrepaal, E., Toet, S., van Logtestijn, R. S., Swart, E., van de Weg, M. J., Callaghan, T. V., & Aerts, R. (2009). Carbon respiration from subsurface peat accelerated by climate warming in the subarctic. *Nature, 460*(7255), 616–619.

Draper, F. C., Roucoux, K. H., Lawson, I. T., Mitchard, E. T., Coronado, E. N. H., Lähteenoja, O., Montenegro, L. T., Sandoval, E. V., Zaráte, R., & Baker, T. R. (2014). The distribution and amount of carbon in the largest peatland complex in Amazonia. *Environmental Research Letters, 9*(12), 124017.

Drexier, J. Z., Bedford, B. L., DeGaetano, A. T., & Siegel, D. I. (1999). Quantification of the water budget and nutrient loading in a small peatland. *JAWRA Journal of the American Water Resources Association, 35*(4), 753–769.

Eva, H. D., Belward, A. S., De Miranda, E. E., Di Bella, C. M., Gond, V., Huber, O., Jones, S., Sgrenzaroli, M., & Fritz, S. (2004). A land cover map of South America. *Global Change Biology, 10*(5), 731–744.

Fang, C., & Moncrieff, J. B. (2001). The dependence of soil $CO_2$ efflux on temperature. *Soil Biology and Biochemistry, 33*(2), 155–165.

Fournier, R. A., Grenier, M., Lavoie, A., & Hélie, R. (2007). Towards a strategy to implement the Canadian Wetland Inventory using satellite remote sensing. *Canadian Journal of Remote Sensing, 33*, S1–S16. http://dx.doi.org/10.5589/m07-051.

Främbs, H. (1994). The importance of habitat structure and food supply for carabid beetles (Coleoptera, Carabidae) in peat bogs. *Memoirs of the Entomological Society of Canada, 126*(S169), 145–159.

Fritz, C., Pancotto, V. A., Elzenga, J. T. M., Visser, E. J. W., Grootjans, A. P., Pol, A., Iturraspe, R., Roelofs, J. G. M., & Smolders, A. J. P. (2011). Zero methane emission bogs: Extreme rhizosphere oxygenation by cushion plants in Patagonia. *New Phytologist, 190*(2), 398–408.

Frolking, S., Roulet, N. T., Moore, T. R., Ball, T., Bellisario, L. M., Bhardwaj, A., Carrol, P., Crill, P. M., Lafleur, P. M., McCaughey, J. H., Suyker, A. E., Verma, S. B., Waddington, J. M., & Whiting, P. J. (1998). Relationship between ecosystem productivity and photosynthetically active radiation for northern peatlands. *Global Biogeochemical Cycles, 12*, 115–126.

Frolking, S., Talbot, J., Jones, M. C., Treat, C. C., Kauffman, J. B., Tuittila, E. S., & Roulet, N. (2011). Peatlands in the Earth's 21st century climate system. *Environmental Reviews, 19*(NA), 371–396.

Fyfe, R. M., Coombe, R., Davies, H., & Parry, L. (2014). The importance of sub-peat carbon storage as shown by data from Dartmoor, UK. *Soil Use and Management, 30*(1), 23–31.

Glaser, P. H. (1981). The patterned mires of the Red Lake peatland, northern Minnesota: Vegetation, water chemistry and landforms. *Journal of Ecology, 69*, 575–599.

Gore, A. J. P. (1983). Introduction. Mires: Swamp, Bog, Fen and Moor. In A. J. P. Gore (Ed.)*, 4A. General studies, ecosystems of the world* (pp. 1–34). Amsterdam: Elsevier.

Gorham, E. (1991). Northern peatlands: Role in the carbon cycle and probable responses to climatic warming. *Ecological Applications, 1*, 182–195.

Graham, J. A., & Vitt, D. H. (2016). The limiting roles of nitrogen and moisture on sphagnum angustifolium growth over a depth to water table gradient. *Plant and Soil, 404*(1), 427–439.

Graham, J. A., Hartsock, J. A., Vitt, D. H., Wieder, R. K., & Gibson, J. J. (2015). Linkages between spatio-temporal patterns of environmental factors and distribution of plant assemblages across a boreal peatland complex. *Boreas, 45*, 207–219.

Grenier, M., Demers, A., Labrecque, S., Benoit, M., Fournier, R. A., & Drolet, B. (2007). An object-based method to map wetland using RADARSAT-1 and Landsat ETM images: Test case on two sites in Quebec, Canada. *Canadian Journal of Remote Sensing, 33*, 528–545.

Gumbricht, T. (2012). *Mapping global tropical wetlands from earth observing satellite imagery (No. CIFOR Working Paper no. 103, p. 47)*. Bogor: Center for International Forestry Research (CIFOR).

Hansen, M. C., Potapov, P. V., Moore, R., Hancher, M., Turubanova, S. A., Tyukavina, A., Thau, D., Stehman, S. V., Goetz, S. J., Loveland, T. R., Kommareddy, A., Egorov, A., Chini, L., Justice, C. O., & Townshend, J. R. G. (2013). High-resolution global maps of 21st-century forest cover change. *Science, 342*, 850–853. Data available on-line from: http://earthenginepartners.appspot.com/science-2013-global-forest.

Harris, A., & Bryant, R. G. (2009). A multi-scale remote sensing approach for monitoring northern peatland hydrology: Present possibilities and future challenges. *Journal of environmental management, 90*(7), 2178–2188.

Henderson, F. M., & Lewis, A. J. (2008). Radar detection of wetland ecosystems: a review. *International Journal of Remote Sensing, 29*(20), 5809–5835.

Hess, L. L., Melack, J. M., Filoso, S., & Wang, Y. (1995). Delineation of inundated area and vegetation along the Amazon floodplain with the SIR-C synthetic aperture radar. *IEEE Transactions on Geoscience and Remote Sensing, 33*(4), 896–904. http://dx.doi.org/10.1109/36.406675.

Hribljan J., Bourgeau-Chavez L. L., Endres S., Suarez E., Lilleskov E. A., Wayson C., Serocki E., and Chimner RA. (2017). Multi-date, multi-sensor remote sensing reveals high density of carbon-rich mountain peatlands in the páramo of Ecuador. *Global Change Biology* 00:1–14. http://dx.doi.org/10.1111/gcb.13807.

Hofstede R, Segarra P, and Mena PV (2003) Los páramos del mundo. Global Peatland Initiative/NC-IUCN/EcoCiencia, Quito 299.

Hooijer, A., Page, S., Jauhiainen, J., Lee, W. A., Lu, X. X., Idris, A., & Anshari, G. (2012). Subsidence and carbon loss in drained tropical peatlands. *Biogeosciences, 9*(3), 1053.
IPCC. (2013). *Climate change 2013. The physical science basis: Working group I contribution to the fifth assessment report of the intergovernmental panel on climate change*. Cambridge University Press.
IPCC. (2014). 2013 Supplement to the 2006 IPCC chapter 2: Drained inland organic soils, guidelines for national greenhouse gas inventories: Wetlands. In T. Hiraishi, T. Krug, K. Tanabe, N. Srivastava, J. Baasansuren, M. Fukuda, & T. G. Troxler (Eds.). Switzerland: IPCC. http://www.ipcc-nggip.iges.or.jp/public/wetlands/.
Joosten, H. (2009). *The global peatland $CO_2$ picture: Peatland status and drainage related emissions in all countries of the world*. Ede: Westland International.
Joosten, H., & Clark, D. (2002). Background and principles including a framework for decision making. Wise use of mires and peatlands. In International Mire Conservation Group and International Peat Society (Ed.). Saarijärvi: NHBS Ltd.
Kimball, J. S., Keyser, A. R., Running, S. W., & Saatchi, S. S. (2000). Regional assessment of boreal forest productivity using an ecological process model and remote sensing parameter maps. *Tree Physiology, 20*(11), 761–775.
Kloiber, S. M., Macleod, R. D., Smith, A. J., Knight, J. F., & Huberty, B. J. (2015). A semi-automated, multi-source data fusion update of a wetland inventory for east-central Minnesota, USA. *Wetlands, 35*(2), 335–348. http://dx.doi.org/10.1007/s13157-014-0621-3.
Koh, L. P., Butler, R. A., & Bradshaw, C. J. (2009). Conversion of Indonesia's peatlands. *Frontiers in Ecology and the Environment, 7*(5), 238.
Koh, L. P., Miettinen, J., Liew, S. C., & Ghazoul, J. (2011). Remotely sensed evidence of tropical peatland conversion to oil palm. *Proceedings of the National Academy of Sciences, 108*(12), 5127–5132.
Kouki, J., Niemi, G. J., & Rajasärkkä, A. (1992). Habitat associations of breeding peatland passerine species in eastern Finland. *Ornis Fennica, 69*, 126–140.
Kuhry, P., & Turunen, J. (2006). Carbon in boreal peatlands. Boreal peatland ecosystems. In R. K. Wieder, & D. H. Vit (Eds.)*, 188*. *Ecological studies: Analysis and synthesis* (pp. 25–40). Berlin: Springer-Verlag.
Lähteenoja, O., Ruokolainen, K., Schulman, L., & Oinonen, M. (2009). Amazonian peatlands: An ignored C sink and potential source. *Global Change Biology, 15*(9), 2311–2320.
Laiho, R. (2006). Decomposition in peatlands: Reconciling seemingly contrasting results on the impacts of lowered water levels. *Soil Biology and Biochemistry, 38*(8), 2011–2024.
Lang, M. W. (2009). Improved detection of forested wetland hydrology with LiDAR intensity. *Wetlands, 29*, 1166–1178.
Lappalainen, E. (Ed.). (1996). Global Peat Resources. In: *International Peat Society*. Finland: Jyväskylä.
Li, J., & Chen, W. (2005). A rule-based method for mapping Canada's wetlands using optical, radar and DEM data. *International Journal of Remote Sensing, 26*(22), 5051–5069.
Limpens, J., Heijmans, M. M., & Berendse, F. (2006). The nitrogen cycle in boreal peatlands. In *Boreal peatland ecosystems* (pp. 195–230). Berlin: Springer.
Limpens, J., Berendse, F., Blodau, C., Canadell, J., Freeman, C., Holden, J., Roulet, N., Rydin, H., & Schaepman-Strub, G. (2008). Peatlands and the carbon cycle: From local processes to global implications–a synthesis. *Biogeosciences, 5*(5), 1475–1491. http://dx.doi.org/10.5194/bg-5-1475-2008.
Lloyd, J., & Taylor, J. A. (1994). On the temperature dependence of soil respiration. *Functional Ecology, 8*(3), 315–323.
Loisel, J., van Bellen, S., Pelletier, L., Talbot, J., Hugelius, G., Karran, D., Yu, Z., Nichols, J., & Holmquist, J. (2017). Insights and issues with estimating northern peatland carbon stocks and fluxes since the Last Glacial Maximum. *Earth-Science Reviews, 165*, 59–80.
Loisel, J., Yu, Z., Beilman, D. W., Camill, P., Alm, J., Amesbury, M. J., Anderson, D., Andersson, S., Bochicchio, C., Barber, K., & Belyea, L. R. (2014). A database and synthesis of northern peatland soil properties and Holocene carbon and nitrogen accumulation. *The Holocene, 24*(9), 1028–1042.
Malmer, N., Svensson, B. M., & Wallén, B. (1994). Interactions between sphagnum mosses and field layer vascular plants in the development of peat-forming systems. *Folia Geobotanica & Phytotaxonomica, 29*(4), 483–496.
Maltby, E., & Proctor, M. C. F. (1996). Peatlands: Their nature and role in the biosphere. In E. Lappalainen (Ed.), *Global peat resources* (pp. 11–19). Jyska: International Peat Society and Geological Survey of Finland.
Margono, B. A., Bwangoy, J. R. B., Potapov, P. V., & Hansen, M. C. (2014). Mapping wetlands in Indonesia using Landsat and PALSAR data-sets and derived topographical indices. *Geo-spatial Information Science, 17*(1), 60–71.
Mazerolle, M. J. (2001). Amphibian activity, movement patterns, and body size in fragmented peat bogs. *Journal of Herpetology, 35*, 13–20.
McGlone, M. S. (2002). The late quaternary peat, vegetation and climate history of the southern oceanic islands of New Zealand. *Quaternary Science Reviews, 21*(4), 683–707.
McLauchlan, K. K., Williams, J. J., Craine, J. M., & Jeffers, E. S. (2013). Changes in global nitrogen cycling during the Holocene epoch. *Nature, 495*(7441), 352–355.
Meehl, G. A., Tebaldi, C., Teng, H., & Peterson, T. C. (2007). Current and future US weather extremes and El Niño. *Geophysical Research Letters, 34*(20), L20704.
Miettinen, J., Shi, C., & Liew, S. C. (2011). Deforestation rates in insular Southeast Asia between 2000 and 2010. *Global Change Biology, 17*(7), 2261–2270.
Miettinen, J., Shi, C., & Liew, S. C. (2016). Land cover distribution in the peatlands of Peninsular Malaysia, Sumatra and Borneo in 2015 with changes since 1990. *Global Ecology and Conservation, 6*, 67–78.
Millard, K., & Richardson, M. (2013). Wetland mapping with LiDAR derivatives, SAR polarimetric decompositions, and LiDAR–SAR fusion using a random forest classifier. *Canadian Journal of Remote Sensing, 39*(4), 290–307.
Millard, K., & Richardson, M. (2015). On the importance of training data sample selection in random forest image classification: A case study in peatland ecosystem mapping. *Remote Sensing, 7*(7), 8489–8515.
Moore, P. D., & Bellamy, D. J. (1974). *Peatlands*. London: Elek.
Moore, T. R., Blodau, C., Turunen, J., Roulet, N., & Richard, P. J. (2005). Patterns of nitrogen and sulfur accumulation and retention in ombrotrophic bogs, eastern Canada. *Global Change Biology, 11*(2), 356–367.
Moore, T. R., Bubier, J. L., Frolking, S. E., Lafleur, P. M., & Roulet, N. T. (2002). Plant biomass and production and $CO_2$ exchange in an ombrotrophic bog. *Journal of Ecology, 90*, 25–36.
Moore, T. R., Bubier, J. L., & Bledzki, L. (2007). Litter decomposition in temperate peatland ecosystems: The effect of substrate and site. *Ecosystems, 10*(6), 949–963.
Moore, T. R., Roulet, N. T., & Waddington, J. M. (1998). Uncertainty in predicting the effect of climatic change on the carbon cycling of Canadian peatlands. *Climatic Change, 40*(2), 229–245.
National Wetlands Working Group (1997) The Canadian Wetland Classification System. In: Warner, BG and Rubec CDA (eds.) *Wetlands Research Centre*, 2nd edn., 68 p. University of Waterloo, Waterloo, ON, Canada.
Olson, C. E. (1960). Elements of photographic interpretation common to several sensors. *Photogrammetric Engineering, 26*(4), 651–656.
Page, S. E., Rieley, J. O., & Wüst, R. (2006). Lowland tropical peatlands of Southeast Asia. *Developments in Earth Surface Processes, 9*, 145–172.
Page, S. E., Rieley, J. O., & Banks, C. J. (2011). Global and regional importance of the tropical peatland carbon pool. *Global Change Biology, 17*(2), 798–818.
Page, S. E., Rieley, J. O., Shotyk, Ø. W., & Weiss, D. (1999). Interdependence of peat and vegetation in a tropical peat swamp forest. *Philosophical Transactions of the Royal Society of London B: Biological Sciences, 354*(1391), 1885–1897.
Posa, M. R. C., Wijedasa, L. S., & Corlett, R. T. (2011). Biodiversity and conservation of tropical peat swamp forests. *BioScience, 61*(1), 49–57.
Poulin, M., Rochefort, L., & Desrochers, A. (1999). Conservation of bog plant species assemblages: Assessing the role of natural remnants in mined sites. *Applied Vegetation Science, 2*(2), 169–180.
Raich, J. W., & Potter, C. S. (1995). Global patterns of carbon dioxide emissions from soils. *Global Biogeochemical Cycles, 9*(1), 23–36.
Rettie, W. J., & Messier, F. (2000). Hierarchical habitat selection by woodland caribou: Its relationship to limiting factors. *Ecography, 23*, 466–478.
Rieley, G., Collier, R., Jones, D., & Eglmton, G. (1996). Ecosystem-specific patterns in the relationship between zooplankton and POM or microplankton 613C. *Geochimica et Cosmochimica Acta, 41*, 777–783.
Ruthsatz, B. (2012). Vegetation and ecology of the high Andean peatlands of Bolivia. *Phytocoenologia, 42*(3–4), 133–179.
Rydin, H., & Jeglum, J. K. (2013). Peatland succession and development. In *The Biology of Peatlands* (pp. 127–147). Oxford, UK: Oxford University Press.
Schmilewski n.d In: Schmilewski G and Rochefort L (Eds) Proceedings of the International Peat Symposium, Pärnu. pp 283–291.

Schuur, E. A., Bockheim, J., Canadell, J. G., Euskirchen, E., Field, C. B., Goryachkin, S. V., Hagemann, S., Kuhry, P., Lafleur, P. M., Lee, H., & Mazhitova, G. (2008). Vulnerability of permafrost carbon to climate change: Implications for the global carbon cycle. *BioScience, 58*(8), 701–714.
See, S. W., Balasubramanian, R., Rianawati, E., Karthikeyan, S., & Streets, D. G. (2007). Characterization and source apportionment of particulate matter $\leq 2.5\ \mu m$ in Sumatra, Indonesia, during a recent peat fire episode. *Environmental science & technology, 41*(10), 3488–3494.
Sklenar, P., & Jorgensen, P. M. (1999). Distribution patterns of paramo plants in Ecuador. *Journal of Biogeography, 26*(4), 681–691.
Smith, A. P., & Young, T. P. (1987). Tropical alpine plant ecology. *Annual Review of Ecology and Systematics, 18*, 137–158.
Smits MJA, Van Duinen GA, Bosman GJCGM, Brock AMT, Javois J, Kuper JT, Peeters TMJ, Peeters MAJ and Esselink J. (2002). Species richness in a species poor system: Aquatic macroinvertebrates of *Nigula raba*, an intact raised bog system in Estonia In: Schmilewski G and Rochefort L (eds.) *Proceedings of the International Peat Symposium*, pp. 283-291. Pärnu.
Steffen, W., Crutzen, P. J., & McNeill, J. R. (2007). The Anthropocene: Are humans now overwhelming the great forces of nature. *AMBIO: A Journal of the Human Environment, 36*(8), 614–621.
Tarnocai, C., Canadell, J. G., Schuur, E. A. G., Kuhry, P., Mazhitova, G., & Zimov, S. (2009). Soil organic carbon pools in the northern circumpolar permafrost region. *Global biogeochemical cycles, 23*(2), 1–9.
Thomas, V., Treitz, P., Jelinski, D., Miller, J., Lafleur, P., & McCaughey, J. H. (2003). Image classification of a northern peatland complex using spectral and plant community data. *Remote sensing of environment, 84*(1), 83–99. http://dx.doi.org/10.1016/s0034-4257(02)00099-8.
Touzi R, Deschamps A, and Rother G (2007) Wetland characterization using polarimetric RADARSAT-2 capability. *Canadian Journal of Remote Sensing* 33(supplement 1) S56–S67.
Turetsky, M. R., Benscoter, B., Page, S., Rein, G., Van Der Werf, G. R., & Watts, A. (2015). Global vulnerability of peatlands to fire and carbon loss. *Nature Geoscience, 8*(1), 11–14.
Turetsky, M. R., Wieder, R. K., Vitt, D. H., Evans, R. J., & Scott, K. D. (2007). The disappearance of relict permafrost in boreal north America: Effects on peatland carbon storage and fluxes. *Global Change Biology, 13*(9), 1922–1934.
Turunen, J., Tomppo, E., Tolonen, K., & Reinikainen, A. (2002). Estimating carbon accumulation rates of undrained mires in Finland–application to boreal and subarctic regions. *The Holocene, 12*(1), 69–80. http://dx.doi.org/10.1191/0959683602hl522rp.
Van der Werf, G. R., Morton, D. C., DeFries, R. S., Olivier, J. G., Kasibhatla, P. S., Jackson, R. B., Collatz, G. J., & Randerson, J. T. (2009). CO2 emissions from forest loss. *Nature Geoscience, 2*(11).
Vitt, D. H. (2006). Functional characteristics and indicators of boreal peatlands. In *Boreal peatland ecosystems* (pp. 9–24). Berlin: Springer.
Vitt, D. H., & Chee, W. L. (1990). The relationships of vegetation to surface water chemistry and peat chemistry in fens of Alberta, Canada. *Vegetatio, 89*, 87–106.
Vitt, D. H., Halsey, L. A., Bray, J., & Kinser, A. (2003). Patterns of bryophyte richness in a complex boreal landscape: Identifying key habitats at McClelland lake wetland. *The Bryologist, 106*(3), 372–382.
Whitcomb, J. B., Moghaddam, M., McDonald, K., Kellndorfer, J., & Podest, E. (2009). Mapping vegetated wetlands of Alaska using L-band radar satellite imagery. *Canadian Journal of Remote Sensing, 35*(1), 54–72. http://dx.doi.org/10.5589/m08-080.
Wieder, R. K., & Lang, G. E. (1983). Net primary production of the dominant bryophytes in a Sphagnum dominated wet land in West Virginia. *The Bryologist, 86*, 280–286.
Wieder, R. K., Vitt, D. H., & Benscoter, B. W. (2006). Peatlands and the boreal forest. In *Boreal peatland ecosystems* (pp. 1–8). Berlin, Heidelberg: Springer.
Wieder, R. K., Scott, K. D., Kamminga, K., Vile, M. A., Vitt, D. H., Bone, T., Xu, B. I. N., Benscoter, B. W., & Bhatti, J. S. (2009). Postfire carbon balance in boreal bogs of Alberta, Canada. *Global Change Biology, 15*(1), 63–81.
Wu, Q., Lane, C., & Liu, H. (2014). An effective method for detecting potential woodland vernal pools using high-resolution LiDAR data and aerial imagery. *Remote Sensing, 6*, 11444–11467.
Yu, Z., Loisel, J., Brosseau, D. P., Beilman, D. W., & Hunt, S. J. (2010). Global peatland dynamics since the last glacial maximum. *Geophysical Research Letters, 37*, L13402.
Yule, C. M. (2010). Loss of biodiversity and ecosystem functioning in Indo-Malayan peat swamp forests. *Biodiversity Conservation, 19*(2), 393–409.
Zoltai, S. C., & Martikainen, P. J. (1996). Estimated extent of forested peatlands and their role in the global carbon cycle. In M. J. Apps, & D. T. Price (Eds.)*, I 40. Forest ecosystems, forest management, and the global carbon cycle, NATO ASI Series* (pp. 47–57). Berlin: Springer-Verlag.
Zoltai, S. C., & Vitt, D. H. (1995). Canadian wetlands: Environmental gradients and classification. *Vegetatio, 118*, 131–137.

## Further Reading

Alemohammad, S.H., Konings, A.G., Jagdhuber, T., Moghaddam, M. and Entekhabi, D., (2016). Characterization of Vegetation and Soil Scattering Mechanisms across Different Biomes using P-band SAR Polarimetry. *arXiv preprint arXiv:1611.02729*.
Beck, P. S., & Goetz, S. J. (2011). Satellite observations of high northern latitude vegetation productivity changes between 1982 and 2008: Ecological variability and regional differences. *Environmental Research Letters, 6*(4), 045501.
Belyea, L. R., & Clymo, R. S. (2001). Feedback control of the rate of peat formation. *Proceedings of the Royal Society of London B: Biological Sciences, 268*(1473), 1315–1321.
Brown, D. G., Johnson, K. M., Loveland, T. R., & Theobald, D. M. (2005). Rural land-use trends in the conterminous United States, 1950–2000. *Ecological Applications, 15*(6), 1851–1863.
Corcoran, J., Knight, J., Brisco, B., Kaya, S., Cull, A., & Murnaghan, K. (2012). The integration of optical, topographic, and radar data for wetland mapping in northern Minnesota. *Canadian Journal of Remote Sensing, 37*(5), 564–582.
Couwenberg, J. (2009). *Emission factors for managed peat soils: An analysis of IPCC default values*. Ede: Wetlands International.
Englhart, S., Keuck, V., & Siegert, F. (2011). Aboveground biomass retrieval in tropical forests-the potential of combined X-and L-band SAR data use. *Remote sensing of environment, 115*(5), 1260–1271.
French, N. H., Kasischke, E. S., Hall, R. J., Murphy, K. A., Verbyla, D. L., Hoy, E. E., & Allen, J. L. (2008). Using Landsat data to assess fire and burn severity in the North American boreal forest region: An overview and summary of results. *International Journal of Wildland Fire, 17*(4), 443–462.
Hribljan, J. A., Lilleskov, E. A., & Chimner, R. A. (2014). Overview of SWAMP protocols for peatland carbon dynamics in the Andes. In *Taller de discussion metodologica caracterizacion de ecosyistemas herbaceous altoandinos y monitoreo de dinamicas de carbona. Quito, Ecuador. 2–3 June 2014*.
Immirzi, C. P., Maltby, E., & Clymo, R. S. (1992). *The global status of peatlands and their role in carbon cycling: A report for Friends of the Earth*. London: Friends of the Earth.
IPCC. (2007). Summary for policymakers. In S. Solomon, D. Qin, M. Manning, Z. Chen, M. Marquis, K. B. Averyt, M. Tignor, & H. L. Miller (Eds.), *Climate change 2007: The physical 13 science basis. Contribution of Working Group I to the Fourth Assessment Report of 14 the Intergovernmental Panel on Climate Change*. Cambridge: Cambridge University Press.
IPCC. (2008). Climate change and water, intergovernmental panel on climate change. In: Bates, B., Kundzewicz, Z. W., Wu, S. and Palutikof, J. (ed.) Technical Paper VI, June 2008.
Ise, T., Dunn, A. L., Wofsy, S. C., & Moorcroft, P. R. (2008). High sensitivity of peat decomposition to climate change through water-table feedback. *Nature Geoscience, 1*(11), 763–766.
Knoth, C., Klein, B., Prinz, T., & Kleinebecker, T. (2013). Unmanned aerial vehicles as innovative remote sensing platforms for high-resolution infrared imagery to support restoration monitoring in cut-over bogs. *Applied vegetation science, 16*(3), 509–517.
Maas, A. (1996). A note on the formation of peat deposits in Indonesia. In *Tropical lowland peatlands of Southeast AsiaProceedings of a workshop on integrated planning and management of tropical lowland peatlands*. Gland, Switzerland: IUCN.

Merchant, M. A., Adams, J. R., Berg, A. A., Baltzer, J. L., Quinton, W. L., & Chasmer, L. E. (2016). Contributions of C-Band SAR data and polarimetric decompositions to subarctic boreal peatland mapping. *IEEE Journal of Selected Topics in Applied Earth Observations and Remote Sensing, 10*, 1467–1482.

Poveda, G., & Pineda, K. (2009). Reassessment of Colombia's tropical glaciers retreat rates: Are they bound to disappear during the 2010–2020 decade? *Advances in Geosciences, 22*, 107.

Reschke, J., Bartsch, A., Schlaffer, S., & Schepaschenko, D. (2012). Capability of C-band SAR for operational wetland monitoring at high latitudes. *Remote Sensing, 4*(10), 2923–2943.

Rieley, J. O., & Ahmad-Shah, A. A. (1996). The extent and nature of tropical peat swamps. In E. Maltyby, C. P. Immirzi, & R. J. Safford (Eds.), *Tropical lowland peatlands of Southeast Asia* (pp. 17–53). Gland: IUCN.

Roulet, N. (2000). Peatlands, carbon storage, greenhouse gases and the Kyoto Protocol: Prospects and significance for Canada. *Wetlands, 20*, 605–615.

Touzi, R., Deschamps, A., & Rother, G. (2009). Phase of target scattering for wetland characterization using polarimetric C-band SAR. *IEEE Transactions on Geoscience and Remote Sensing, 47*(9), 3241–3261.

Touzi, R., Deschamps, A., & Rother, G. (2008). Scattering type phase for wetland classification using C-band polarimetric SAR. In *Geoscience and Remote Sensing Symposium, 2008. IGARSS, IEEE International. 2* pp. 285–288).

Tarnocai, C. (2006). The effect of climate change on carbon in Canadian peatlands. *Global and planetary Change, 53*(4), 222–232.

Thompson, D. K., Simpson, B. N., & Beaudoin, A. (2016). Using forest structure to predict the distribution of treed boreal peatlands in Canada. *Forest Ecology and Management, 372*, 19–27.

Truong-Loi, M. L., Dubois-Fernandez, P., & Pottier, E. (2012). Assessment of forest biomass retrieval from compact-pol SAR data. *Canadian Journal of Remote Sensing, 38*(4), 452–460.

Turetsky, M. R., Wieder, R. K., & Vitt, D. H. (2002). Boreal peatland C fluxes under varying permafrost regimes. *Soil Biology and Biochemistry, 34*(7), 907–912.

Vasander, H., & Kettunen, A. (2006). Carbon in boreal peatlands. In *Boreal peatland ecosystems* (pp. 165–194). Berlin, Heidelberg: Springer.

Vitt, D. H., Li, Y., & Belland, R. J. (1995). Patterns of bryophyte diversity in peatlands of continental western Canada. *Bryologist, 98*(2), 218–227. http://dx.doi.org/10.2307/3243306.

Wheeler, B. D., & Proctor, M. C. F. (2000). Ecological gradients, subdivisions and terminology of north-west European mires. *Journal of ecology, 88*(2), 187–203.

Whitcomb, J. B., Moghaddam, M., McDonald, K., Podest, E., & Chapman, B. (2008). Decadal change in Northern Wetlands based on analysis of ALOS/PALSAR and JERS SAR data. In *AGU Fall Meeting Abstracts*.

From Bourgeau-Chavez, L. L., Endres, S. L., Graham, J. A., Hribljan, J. A., Chimner, R. A., Lillieskov, E. A., & Battaglia, M. J. (2018) Mapping Peatlands in Boreal and Tropical Ecoregions. In S. Liang (Ed.), Comprehensive Remote Sensing, vol. 6, pp. 24–44.
Oxford: Elsevier.
ISBN: 9780128032206